

Multi-user lattice coding for the multiple-access relay channel

Chung-Pi Lee, Shih-Chun Lin, Hsuan-Jung Su and H. Vincent Poor

Abstract

This paper considers the multi-antenna multiple access relay channel (MARC), in which multiple users transmit messages to a common destination with the assistance of a relay. In a variety of MARC settings, the dynamic decode and forward (DDF) protocol is very useful due to its outstanding rate performance. However, the lack of good structured codebooks so far hinders practical applications of DDF for MARC. In this work, two classes of structured MARC codes are proposed: 1) one-to-one relay-mapper aided multiuser lattice coding (O-MLC), and 2) modulo-sum relay-mapper aided multiuser lattice coding (MS-MLC). The former enjoys better rate performance, while the latter provides more flexibility to tradeoff between the complexity of the relay mapper and the rate performance. It is shown that, in order to approach the rate performance achievable by an unstructured codebook with maximum-likelihood decoding, it is crucial to use a new K -stage coset decoder for structured O-MLC, instead of the one-stage decoder proposed in previous works. However, if O-MLC is decoded with the one-stage decoder only, it can still achieve the optimal DDF diversity-multiplexing gain tradeoff in the high signal-to-noise ratio regime. As for MS-MLC, its rate performance can approach that of the O-MLC by increasing the complexity of the modulo-sum relay-mapper. Finally, for practical implementations of both O-MLC and MS-MLC, practical short length lattice codes with linear mappers are designed, which facilitate efficient lattice decoding. Simulation results show that the proposed coding schemes outperform existing schemes in terms of outage probabilities in a variety of channel settings.

I. INTRODUCTION

In recent years, cooperative communication has drawn a significant amount of interest as a means of providing spatial diversity when time, frequency or antenna diversities are unavailable due to delay, bandwidth or terminal size constraints, respectively. Cooperative communication techniques for single-source networks have been extensively studied in terms of rate, outage probability or diversity-multiplexing

C.-P. Lee and H.-J. Su are with Department of Electrical Engineering and Graduate Institute of Communication Engineering, National Taiwan University, Taipei, Taiwan, 10617. S.-C. Lin is with the Department of Electronic and Computer Engineering, National Taiwan University of Science and Technology, Taipei, Taiwan, 10607. H. V. Poor is with the Department of Electrical Engineering, Princeton University, Princeton, NJ, 08544, USA. Emails: {D96942016@ntu.edu.tw, sclin@mail.ntust.edu.tw, hjsu@cc.ee.ntu.edu.tw, poor@princeton.edu}.

tradeoff (DMT) perspectives [1] [2] [3]. However, practical communication networks usually involve more than one source (user), leading to the study of the multiple-access channel (MAC). In this paper, we consider an important multi-user cooperative communication channel, that is, the multi-antenna multiple-access relay channel (MARC). The MARC is a MAC with an additional shared half-duplex relay [4]. It has been shown that the MARC provides a much larger achievable rate region [4] and diversity gain per user [5], compared to those of the MAC. Also, since a single relay is shared by multiple users in the MARC, the extra cost of adding such a relay is acceptable. However, the code design for the MARC needs to jointly consider the codebooks of the multiple users and the relay [4] [6] [7], and is thus not a trivial extension of those for the single-user relay channel or the multiple access channel.

The achievable rate region of the MARC has been characterized in [4] [6] and [7]. The decode and forward protocol, which is a special case of the dynamic decode and forward (DDF) protocol [8], was shown to achieve the capacity region of the MARC when the source-relay link is good enough [7], thus having a larger achievable rate region than those of the multiple-access amplify and forward (MAF) [5] and compress and forward (CF) protocols [9]. However, the capacity region of the general MARC remains unknown. The DMT for the MARC with single antenna nodes was studied in [5] [8] and [9]. Although the MAF and CF are both DMT optimal in the high multiplexing gain regime [5] [9], compared with the DDF strategy, they both achieve lower diversity gains in the low to medium multiplexing gain regimes [5] [9]. Moreover, in [5], simulation results show that the DDF protocol yields a better outage probability than that of MAF and CF over a large range of signal-to-noise ratio (SNR), even at the high multiplexing gain regime. Thus we focus on the DDF in this paper due to its good performance in a variety of operation settings.

However, previous results in [4]–[9] are based on *unstructured* random codebooks and maximum likelihood (ML) decoders, and are very difficult to implement in practice. In this paper, we propose *structured* multiuser lattice coding aided by a relay mapper for the MARC under the DDF protocol, in which each node in the MARC has multiple antennas. To simplify the joint codebook design problem for the multiple users and the relay, we introduce a relay mapper which selects the codeword to be transmitted at the relay to aid the users' transmissions. The relay mapper is a key new ingredient for our coding design, which can also help implement the unstructured codebooks in [4], [6], [7] and [8] in practice, and does

not appear in [4]–[9]. However, the introduction of the relay mapper makes the decoding much more difficult than that for the MAC [10]. We will see that the one-stage coset decoding proposed in [10] fails to achieve the rate performance of the unstructured codebook with the ML decoding demonstrated in [7]. Instead, we propose a new K -stage coset decoder that achieves the rate performance in [7] by successive cancellation on the multiuser decoding tree. Two classes of relay mapper aided multiuser lattice coding are proposed: 1) one-to-one relay mapper aided multiuser lattice coding (O-MLC), and 2) modulo-sum relay mapper aided multiuser lattice coding (MS-MLC). The first enjoys better rate performance while the second provides more flexibility to tradeoff between the complexity of the relay mapper and the rate performance. With the K -stage coset decoder, the structured O-MLC can achieve the rate performance obtained by the unstructured codebook in [7]. If only one-stage coset decoding is used, we also show that O-MLC is DMT optimal for the DDF, and has better DMT than that in [5] and [9] for the low to medium multiplexing gain regime. As for MS-MLC, when the codomain size of the modulo-sum relay mapper becomes larger, the error performance of MS-MLC approaches that of O-MLC. Moreover, our decoder is no longer a simple lattice decoder as that of [10], since the lattice structure for decoding may be destroyed by the relay mapper. Further, a naive application of the theoretical error analysis in [10] suffers from significant losses in prediction of the achievable rates of proposed coding. We overcome this problem by introducing a new technique for bounding the error probability over the random relay-mapper codebook ensemble. Finally, to implement our theoretical results, we construct practical lattice codebooks with *linear* mappings for both O-MLC and MS-MLC, which enable the decoder to use the efficient lattice decoding algorithms in [11] and [12].

Compared with codes appearing in previous works [4], [6]–[9] which are difficult to implement, our structured MARC coding can be implemented in practice as we will see below. Some practical MARC code designs were proposed in [13] and [14], but these studies lack theoretical performance analysis. In [13] and [14], an orthogonal protocol was used in which users and the relay must transmitted in different time slots to avoid interference, while our scheme allows them to transmit simultaneously. Moreover, in [14], instead of joint code design, the relay’s transmitted symbol is formed from the users’ symbols with a simple transformation. Due to the above reasons, there are significant losses in the achievable rates and DMTs for the methods in [13] and [14], compared with our schemes. In simulations, we show that our

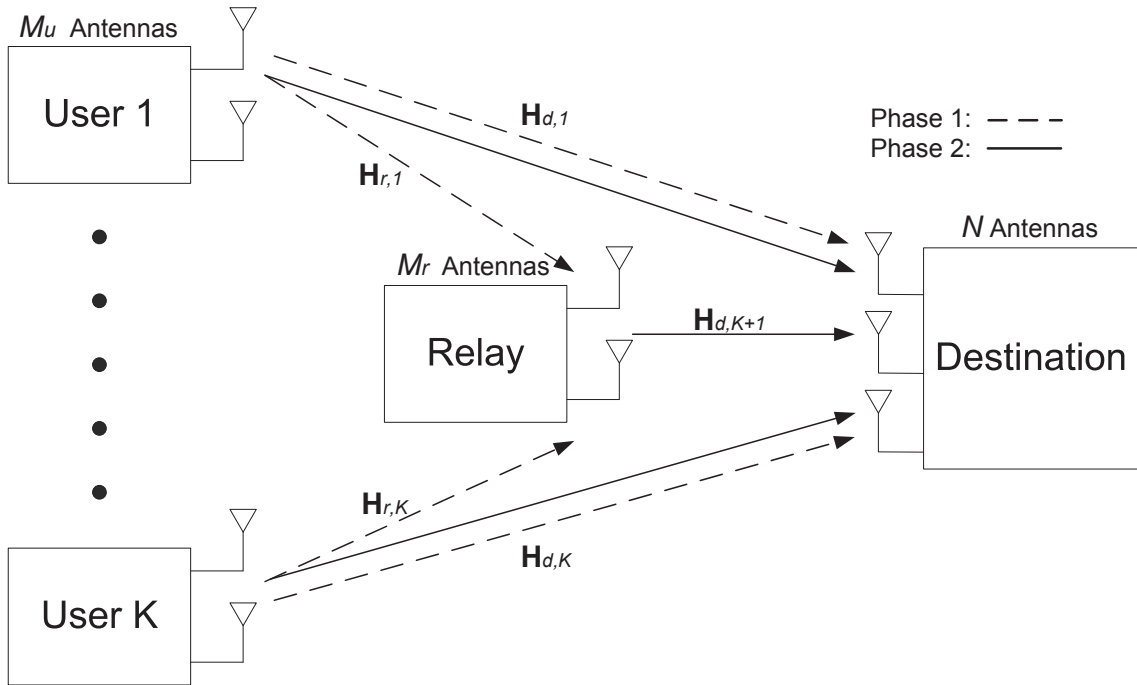


Fig. 1. Dynamic decode and forward (DDF) for the K -user multiple-antenna multiple-access relay channel (MARC), where Phase 1 is the relay's listening phase while Phase 2 is the relay's transmitting phase.

proposed lattice coding schemes also outperform the schemes in [5] [9] [13] and [14] in terms of outage probabilities.

The rest of this paper is organized as follows. Section II introduces the system model and some frequently used notation is summarized in Table I. In Section III, O-MLC and MS-MLC are introduced. In Section IV, we establish the achievable rate region for both O-MLC and MS-MLC and show that O-MLC is DMT optimal. In Section V, simulation results are presented, and Section VI concludes the paper.

II. SYSTEM MODEL

We consider the K -user multiple-antenna MARC as shown in Fig. 1, in which a relay node is assigned to assist the multiple-access users in transmitting data to a common destination. Each user and the relay is equipped with M_u and M_r antennas, respectively, and the destination has N antennas. In the DDF for MARC, each codeword spans L slots each consisting of T vector symbols, and the block of LT vector

symbols is split into two phases due to the half-duplex constraint at the relay node (i.e., it cannot transmit and receive simultaneously). In Phase 1, the relay receives the signals from the users, then it tries to decode the users' messages until the decision time $\ell_1 T$. Following [8], $\ell_1 T$ is chosen to be the earliest time index such that after $\ell_1 T$ symbols, the relay can decode the users' messages without error. If there is no such $\ell_1 \in \{1, \dots, L-1\}$, the relay remains silent. Let the $M_r \times M_u$, $N \times M_u$ channel matrices from user i to the relay and the destination be $\mathbf{H}_{r,i}$ and $\mathbf{H}_{d,i}$, respectively, which are perfectly known at the corresponding receivers. For Phase 1, the received $M_r \times 1$ vector of symbols at the relay is*

$$\mathbf{y}_{r,l} = \sqrt{\frac{\rho_r}{M_u}} \sum_{i=1}^K \mathbf{H}_{r,i} \mathbf{x}_{i,l} + \mathbf{n}_l, \quad l = 1, 2, \dots, \ell_1 T \quad (1)$$

where ρ_r is the received SNR at the relay, $\mathbf{x}_{i,l}$ is the $M_u \times 1$ vector signal transmitted by user i at time index l , and the noise at the relay $\mathbf{n}_l \sim \mathcal{CN}(\mathbf{0}, \mathbf{I}_{M_r})$ is a Gaussian vector with independent and identically distributed (i.i.d.) entries. Similar to (1), the received vector symbols at the destination in Phase 1 is

$$\mathbf{y}_{d_1,l} = \sqrt{\frac{\rho_d}{M_u}} \sum_{i=1}^K \mathbf{H}_{d,i} \mathbf{x}_{i,l} + \mathbf{v}_l, \quad l = 1, 2, \dots, \ell_1 T \quad (2)$$

where ρ_d is the received SNR and $\mathbf{v}_l \sim \mathcal{CN}(\mathbf{0}, \mathbf{I}_N)$ is the noise vector at the destination. In Phase 2 of DDF, based on the decoded messages obtained at the decision time $\ell_1 T$, the relay transmits the corresponding coded vector symbols to the destination. The signal received by the destination is then

$$\mathbf{y}_{d_2,l} = \sqrt{\frac{\rho_d}{M_u}} \sum_{i=1}^K \mathbf{H}_{d,i} \mathbf{x}_{i,l} + \sqrt{\frac{\rho_d}{M_r}} \mathbf{H}_{d,K+1} \mathbf{x}_{K+1,l} + \mathbf{v}_l, \quad l = \ell_1 T + 1, \ell_1 T + 2, \dots, LT \quad (3)$$

where $\mathbf{x}_{K+1,l}$ denotes for the signal transmitted by the relay and $\mathbf{H}_{d,K+1}$ is the channel matrix from the relay to destination. As for the (normalized) MARC input power constraint, it is imposed on each user and the relay as

$$E \left[\frac{1}{LT} \sum_{l=1}^{LT} |\mathbf{x}_{i,l}|^2 \right] \leq M_u, \quad E \left[\frac{1}{LT} \sum_{l=1}^{LT} |\mathbf{x}_{K+1,l}|^2 \right] \leq M_r, \quad i = 1, \dots, K \quad (4)$$

where the expectation $E[\cdot]$ is taken over all codewords in the codebook.

***Notation:** Let A be a set, then $A^* = A \setminus \{\mathbf{0}\}$. A^c denotes the complement of A , and $|A|$ denotes the cardinality of A . For a matrix \mathbf{M} , \mathbf{M}^H is the conjugate transpose and $|\mathbf{M}|$ is the determinant. We use $\log(\cdot)$ for the logarithm with base 2, and \times for the direct product. An n -dimensional real lattice Λ is a discrete additive subgroup of \mathbb{R}^n . The lattice quantization function is defined as $Q_\Lambda(\mathbf{y}) \triangleq \arg \min_{\lambda \in \Lambda} |\mathbf{y} - \lambda|$ for $\mathbf{y} \in \mathbb{R}^n$, and the modulo-lattice operation $\bar{\mathbf{y}} = \mathbf{y} \bmod \Lambda \triangleq \mathbf{y} - Q_\Lambda(\mathbf{y})$ [15]. The second-order moment of Λ is defined as $\sigma^2(\Lambda) \triangleq \frac{1}{nV_f(\Lambda)} \int_{\mathcal{V}_\Lambda} \mathbf{x}^2 d\mathbf{x}$, where \mathcal{V}_Λ and $V_f(\Lambda)$ are given in (T1.2) and (T1.3) in Table I, respectively. Some other frequently used notation is also summarized in Table I.

To simplify the presentation for the proposed lattice coding scheme, it is useful to transform our received signal model (1), (2) and (3) into the equivalent real channel model form as in (5) and (6), for the relay and the destination, respectively,

$$\mathbf{y}_{relay} = \mathbf{H}_{relay}\mathbf{x}_{relay} + \mathbf{n}_{relay} \quad (5)$$

$$\mathbf{y}_{dst} = \mathbf{H}_{dst}\mathbf{x}_{dst} + \mathbf{n}_{dst}. \quad (6)$$

The equivalent channel for the destination (6) is formed by concatenating the received signal (2) in Phase 1 and (3) in Phase 2, and the $2(KM_u + M_r)LT \times 1$ super signal vector \mathbf{x}_{dst} in (6) is

$$\mathbf{x}_{dst} \triangleq [\mathbf{x}_1^T, \dots, \mathbf{x}_{K+1}^T]^T, \quad (7)$$

where $\mathbf{x}_i = [\{\mathbf{x}_{i,1}^R\}^T, \dots, \{\mathbf{x}_{i,LT}^R\}^T]^T$ with $\mathbf{x}_{i,l}^R = [\text{Re}\{\mathbf{x}_{i,l}\}^T, \text{Im}\{\mathbf{x}_{i,l}\}^T]^T$; while the $2NLT \times 1$ super received signal and noise at the destination \mathbf{y}_{dst} and \mathbf{n}_{dst} in (6) are similarly defined respectively. The $2NLT \times 2(KM_u + M_r)LT$ super-channel matrix \mathbf{H}_{dst} in (6) is $\mathbf{H}_{dst} \triangleq [\mathbf{H}_1^d, \dots, \mathbf{H}_{K+1}^d]$, where the $2NLT \times 2M_uLT$ equivalent channel matrix \mathbf{H}_i^d for user i comes from (2) as

$$\mathbf{H}_i^d \triangleq \sqrt{\frac{\rho_d}{M_u}} \mathbf{I}_{LT} \otimes \begin{pmatrix} \text{Re}\{\mathbf{H}_{d,i}\} & -\text{Im}\{\mathbf{H}_{d,i}\} \\ \text{Im}\{\mathbf{H}_{d,i}\} & \text{Re}\{\mathbf{H}_{d,i}\} \end{pmatrix} \quad (8)$$

where \otimes denotes the Kronecker product and $i = 1, \dots, K$, while the equivalent channel matrix \mathbf{H}_{K+1} for the relay comes from (3) as

$$\mathbf{H}_{K+1}^d \triangleq \text{diag} \left(\mathbf{I}_{\ell_1 T} \otimes \mathbf{0}_{2N \times 2M_r}, \sqrt{\frac{\rho_d}{M_r}} \mathbf{I}_{(L-\ell_1)T} \otimes \begin{pmatrix} \text{Re}\{\mathbf{H}_{d,K+1}\} & -\text{Im}\{\mathbf{H}_{d,K+1}\} \\ \text{Im}\{\mathbf{H}_{d,K+1}\} & \text{Re}\{\mathbf{H}_{d,K+1}\} \end{pmatrix} \right), \quad (9)$$

if $1 \leq \ell_1 \leq L-1$, where the first $2N\ell_1 T \times 2M_r\ell_1 T$ is a zero matrix because the relay is listening in Phase 1 (if $\ell_1 = L$, $\mathbf{H}_{K+1}^d \triangleq \mathbf{0}_{2NLT \times 2M_rLT}$ since the relay is silent). As for the equivalent channel for the relay (5), it can be similarly obtained from (1) as above, with the dimensions of \mathbf{H}_{relay} being $2M_rLT \times 2KM_uLT$. We consider two kinds of channel settings, the fixed channel and the slow fading channel. In the fixed channel setting, the channels are deterministic and we use the achievable rate as a performance metric. For the slow fading channel, \mathbf{H}_{dst} and \mathbf{H}_{relay} are random but remain constant over the whole code block. Since the MARC cannot support any non-zero rate pairs with vanishing error probabilities now, we use the DMT or the outage probabilities as performance metrics. The entries of the channel matrices are assumed to be i.i.d. $\mathcal{CN}(0,1)$ when they are slow faded; i.e., we assume Rayleigh fading in this case.

III. PROPOSED RELAY-MAPPER AIDED MULTIUSER LATTICE CODING SCHEMES

In this section, we specify the proposed multiuser lattice coding schemes for the MARC, i.e., O-MLC and MS-MLC. Each of O-MLC and MS-MLC consists of three building blocks: 1) the relay mapper which decides which codeword to be transmitted at the relay, 2) Loeliger-type nested lattices for the users' and the relay's codebooks and 3) a K -stage coset decoder, which generalizes the one-stage decoder of [10]. We first briefly introduce the adopted lattice codebooks. Tailored for them, the relay mappers, the one-to-one mapper ψ^{one} and the modulo-sum mapper ψ^{mod} , for O-MLC and MS-MLC, respectively are shown in Section III-B. Then the whole encoding/decoding blocks are introduced in Section III-C.

A. Loeliger-type Nested Lattice Codebooks

In our code construction, codebooks of the i -th user ($1 \leq i \leq K$) and the relay ($i = K + 1$) are generated from Loeliger-type nested lattices. To be specific, we introduce the following definitions.

Definition 1 (Self-similar nested lattice code): For user i , let Λ_{C_i} be a $2M_u LT$ -dimensional coding lattice and $\Lambda_{S_i} \subset \Lambda_{C_i}$ be the shaping lattice. The nested lattice codebook is defined as $C_i^{nest} \triangleq \{\bar{\mathbf{c}}_i : \bar{\mathbf{c}}_i = \mathbf{c}_i \bmod \Lambda_{S_i}, \mathbf{c}_i \in \Lambda_{C_i}\}$, where $\bar{\mathbf{c}}_i$ are the coset leaders [15] of the partition $\Lambda_{C_i}/\Lambda_{S_i}$ (the set of cosets of Λ_{S_i} relative to Λ_{C_i}). The codebook size is $|C_i^{nest}| = 2^{R_i LT}$, where the code rate is R_i bits per channel use (BPCU). When $\Lambda_{S_i} = (2^{R_i/2M_u})\Lambda_{C_i}$ where $(2^{R_i/2M_u}) \in \mathbb{N}$ is the nesting ratio, the nested lattice code C_i^{nest} is called a self-similar nested code.[†]

For a Loeliger-type nested-lattice ensemble, the coding lattice Λ_{C_i} for user i is randomly chosen from the Loeliger lattices ensemble which is generated from linear codes C_i^{Lo} [17]. The detailed definition is given in Definition 5 in the Appendix A-(I).

The codebook for the relay is generated similarly as above but with dimension $2M_r LT$.

B. Proposed Relay Mappers

The relay mapper ψ is used to select the codeword (coset leader) $\bar{\mathbf{c}}_{K+1}$ to be transmitted from the relay (transmitter $K + 1$) according to the codewords (coset leaders) $\bar{\mathbf{c}}_i$, $i = 1, \dots, K$, of the K users. In other words, by concatenating the total $K + 1$ codewords as a super one $\bar{\mathbf{c}} = [(\bar{\mathbf{c}}_1^T, \dots, \bar{\mathbf{c}}_K^T), \bar{\mathbf{c}}_{K+1}^T]^T = [\bar{\mathbf{c}}_u^T, \bar{\mathbf{c}}_r^T]^T$ ((T1.5) in Table I), then $\psi(\bar{\mathbf{c}}_u) = \bar{\mathbf{c}}_r$. Now we introduce the proposed mappers. The first one is as follows.

Definition 2 (One-to-one mapper): The one-to-one mapper $\psi^{one} : C_u^{nest} \rightarrow C_r^{nest}$ for O-MLC is a one-to-one bijective mapping that maps coset leaders in the super-codebook of users C_u^{nest} to the relay codebook

[†] Our results can be easily generalized to the case in which good (but maybe not self-similar) nested codes as in [16] are used.

TABLE I
LIST OF FREQUENTLY USED NOTATION

Notation	Definition	Description
(T1.1) \mathbb{Z}_p^n	n -dimensional finite field over $\mathbb{Z}_p = \{0, 1, \dots, p-1\}$, where p is a prime	Prime p finite field
(T1.2) \mathcal{V}_Λ	The set of $\mathbf{v} \in \mathbb{R}^n$ closer to $\mathbf{0}$ than to any other $\lambda \in \Lambda$, for a lattice Λ	Voronoi Region
(T1.3) $V_f(\Lambda)$	Volume of Voronoi region \mathcal{V}_Λ in (T1.2)	Fundamental Volume
(T1.4) \mathbf{v}_i	$n_i \times 1$ vector $\mathbf{v}_i \in \Lambda_i$ consists of the elements of \mathbf{v} in Λ_i , where $\mathbf{v} = [\mathbf{v}_1^T, \dots, \mathbf{v}_{K+1}^T]^T$ is $(\sum_{i=1}^{K+1} n_i) \times 1$, and Λ_i is transmitter i 's lattice (coding or shaping)	Vector for transmitter i , where $1 \leq i \leq K$ correspond to the users while $i = K+1$ corresponds to the relay
(T1.5) $\mathbf{v}_u, \mathbf{v}_r$	$\mathbf{v}_u = [\mathbf{v}_1^T, \dots, \mathbf{v}_K^T]^T$, $\mathbf{v}_r = \mathbf{v}_{K+1}$, with \mathbf{v}_i defined in (T1.4)	Super-vector for all users, and vector for relay
(T1.6) C_{ur}^{Lo}	$C_1^{Lo} \times \dots \times C_{K+1}^{Lo}$, where C_i^{Lo} is the Loeliger linear code for transmitter i as in Definition 5	Super Loeliger-linear-code of users and relay
(T1.7) $\Lambda_{C_u}, \Lambda_{S_u}$	$\Lambda_{C_1} \times \dots \times \Lambda_{C_K}, \Lambda_{S_1} \times \dots \times \Lambda_{S_K}$	Super-coding and shaping lattices of users
(T1.8) $\Lambda_{C_r}, \Lambda_{S_r}$	$\Lambda_{C_{K+1}}, \Lambda_{S_{K+1}}$	Super-coding and shaping lattices of relay
(T1.9) $\Lambda_{C_{ur}}, \Lambda_{S_{ur}}$	$\Lambda_{C_1} \times \dots \times \Lambda_{C_{K+1}}, \Lambda_{S_1} \times \dots \times \Lambda_{S_{K+1}}$	Super-coding and shaping lattices of users and relay
(T1.10) $\bar{\mathbf{v}}, \bar{\mathbf{v}}_i$	$\mathbf{v} \bmod \Lambda_{S_{ur}}, \mathbf{v}_i \bmod \Lambda_{S_i}$	Modulo lattice operation
(T1.11) p_i, γ_i	Definition 5	Loeliger lattice ensemble parameters
(T1.12) Ψ^{one}, Ψ^{mod}	Definition 2, 3	One-to-one Mapper, Modulo-sum Mapper
(T1.13) C_u^{nest}, C_r^{nest}	Definition 2	Users' Codebooks, Relay's Codebook
(T1.14) $\Psi_\Delta^{one}, \Psi_\Delta^{mod}$	$\Psi_\Delta^{one} : \Psi_\Delta^{one}(\bar{\mathbf{d}}_u(\mathbf{w})) = \bar{\mathbf{d}}_r(\mathbf{w}), \Psi_\Delta^{mod} : \Psi_\Delta^{mod}(\bar{\mathbf{d}}_u(\mathbf{w})) = \bar{\mathbf{d}}_r(\mathbf{w})$	Differential mapper for one-to-one and modulo-sum mapper
(T1.15) $(C_{C_{\Psi_\Delta, E}})^*$	$(C_{C_{\Psi_\Delta, E}})^* \triangleq \{\bar{\mathbf{d}} : \bar{\mathbf{d}} \in C_{\Psi_\Delta}^*, C_{\Psi_\Delta} \in C_{\Psi_\Delta, E}\}$	Differential codewords in ensemble $C_{\Psi_\Delta, E}$
(T1.16) $\mathcal{O}^{\Psi_\Delta}$	(13)	Differential ambiguity cosets
(T1.17) \mathbf{M}^S	Matrix $\mathbf{M}^S \triangleq [\mathbf{M}_{i_1}, \dots, \mathbf{M}_{i_{ S }}]$ is formed from $\mathbf{M} = [\mathbf{M}_1, \dots, \mathbf{M}_{K_M}]$, where K_M is the number of the submatrices of \mathbf{M} , $S = \{i_1, \dots, i_{ S }\}$, $1 \leq i_1 < \dots < i_{ S } \leq K_M$	Matrix for users in set S
(T1.18) $R_{unG}^{dst}(\mathbf{H}_{dst}^{\{S, K+1\}})$	$\frac{1}{2} \log \mathbf{I}_{2(S M_u + M_r)LT} + (\mathbf{H}_{dst}^{\{S, K+1\}})^H \mathbf{H}_{dst}^{\{S, K+1\}} $	Rate constraint at the destination using unstructured Gaussian codebook
(T1.19) $R_{unG}^{relay}(\mathbf{H}_{relay}^S)$	$\frac{1}{2} \log \mathbf{I}_{2 S M_u LT} + (\mathbf{H}_{relay}^S)^H \mathbf{H}_{relay}^S $	Rate constraint at the relay using unstructured Gaussian codebook
(T1.20) $d(\mathbf{r})$	The diversity gain $\lim_{\rho \rightarrow \infty} \frac{-\log P_E(\rho)}{\log \rho}$ given a certain multiplexing gain \mathbf{r} , where $P_E(\rho)^\S$ is the probability that not all users are correctly decoded, ρ is the received SNR, and $\mathbf{r} = [r_1, \dots, r_K]$ with $r_i \triangleq \lim_{\rho \rightarrow \infty} \frac{R_i(\rho)}{\log \rho}$ and $R_i(\rho)$ is the transmission rate of user i	Diversity and multiplexing tradeoff (DMT)
(T1.21) $\bar{\mathbf{z}}_p$	Apply componentwise modulo p operation on \mathbf{z}	Modulo p
(T1.22) $\bar{\mathbf{z}}_{\underline{p}}$	$[(\bar{\mathbf{z}}_1)_{p_1}^T, \dots, (\bar{\mathbf{z}}_1)_{p_{K+1}}^T]$, for $\underline{p} = (p_1, \dots, p_{K+1})$, $\mathbf{z} = [\mathbf{z}_1^T, \dots, \mathbf{z}_{K+1}^T]^T$	Modulo vector \underline{p}
(T1.23) $\underline{\gamma} \mathbf{z}$	$[\gamma_1 \mathbf{z}_1^T, \dots, \gamma_{K+1} \mathbf{z}_{K+1}^T]^T$, for $\underline{\gamma} = (\gamma_1, \dots, \gamma_{K+1})$, $\mathbf{z} = [\mathbf{z}_1^T, \dots, \mathbf{z}_{K+1}^T]^T$	"Vector" Hadamard product

^{\S} Instead of $P_E(\rho)$, the outage probability is used for the calculation of DMT of the relay node in the DDF [3], [8]

C_r^{nest} . Here $C_u^{nest} \triangleq \{\bar{\mathbf{c}}_u : \bar{\mathbf{c}}_u = (\mathbf{c}_u \bmod \Lambda_{S_u}), \mathbf{c}_u \in \Lambda_{C_u}\}$ and $C_r^{nest} \triangleq \{\bar{\mathbf{c}}_r : \bar{\mathbf{c}}_r = (\mathbf{c}_r \bmod \Lambda_{S_r}), \mathbf{c}_r \in \Lambda_{C_r}\}$, where Λ_{S_u} and Λ_{C_u} are defined in (T1.7) while Λ_{S_r} and Λ_{C_r} are defined in (T1.8) in Table I.

Note that $|C_r^{nest}| = |C_u^{nest}|$ since the aforementioned mapping is bijective. The one-to-one relay mapper may require high complexity as the size of super-user codebook $|C_u^{nest}|$ becomes large. To reduce the complexity of the mapper, we introduce another mapping ψ^{mod} , where the modulo-sum operation is performed at the relay, which is motivated by the XOR operations in network coding [18].

Definition 3 (Modulo-sum mapper): The modulo-sum mapper $\psi^{mod} : C_u^{nest} \rightarrow C_r^{nest}$ for MS-MLC is defined as $\psi^{mod}(\bar{\mathbf{c}}_u) = \sum_{i=1}^K \psi_i^{mod}(\bar{\mathbf{c}}_i) \bmod \Lambda_{S_r}$, where $\psi_i^{mod} : C_i^{nest} \rightarrow C_r^{nest}$ is an injective mapping for user i with nested user codebook C_i^{nest} given in Definition 1, while C_u^{nest} and C_r^{nest} are given in Definition 2.

Note we require that $|C_r^{nest}| \geq \max_i\{|C_i^{nest}|\}$ to ensure that the mapping ψ_i^{mod} in Definition 3 is injective. The domain dimension of ψ^{mod} is at most $\max_i\{|C_i^{nest}|\}$ while that of the one-to-one mapper ψ^{one} is $\prod_{i=1}^K |C_i^{nest}|$, and ψ^{mod} has less complexity compared with ψ^{one} . However, the one-to-one mapper ψ^{one} ensures that two different users' super-codewords are mapped to different codewords at the relay, and results in better error performance. In contrast, it is possible that two different super-codewords map to the same codeword of the relay due to the modulo-sum operation in ψ^{mod} , and ambiguity occurs while decoding.

C. Encoders and Proposed K -stage Coset Decoders

1) *Encoders at the K transmitters and the relay:* User i selects the codeword $\bar{\mathbf{c}}_i$ according to its message w_i from the codebook described in Section III-A, and sends signal \mathbf{x}_i into the MARC (5)-(6) (cf. (7))

$$\mathbf{x}_i = ([\bar{\mathbf{c}}_i - \mathbf{u}_i] \bmod \Lambda_{S_i}) \quad (10)$$

where \mathbf{u}_i is a dither signal uniformly distributed over the Voronoi region $\mathcal{V}_{\Lambda_{S_i}}$ of the shaping lattice Λ_{S_i} ((T1.2) in Table I). From [19], due to the dither \mathbf{u}_i , \mathbf{x}_i is uniformly distributed over $\mathcal{V}_{\Lambda_{S_i}}$ and independent of $\bar{\mathbf{c}}_i$. To meet the input power constraints (4) as in [16], we let the second-order moment of the shaping lattice $\sigma^2(\Lambda_{S_i}) = 1/2$.

As for the relay (transmitter $K+1$), it will first decode the users' messages, using the operation introduced below. Then the relay selects its codeword $\bar{\mathbf{c}}_{K+1}$ according to the decoded transmitted codewords $\bar{\mathbf{c}}_i$ s using the mappers in Section III-B, and then transmits \mathbf{x}_{K+1} as in (10) with the power constraint (4).

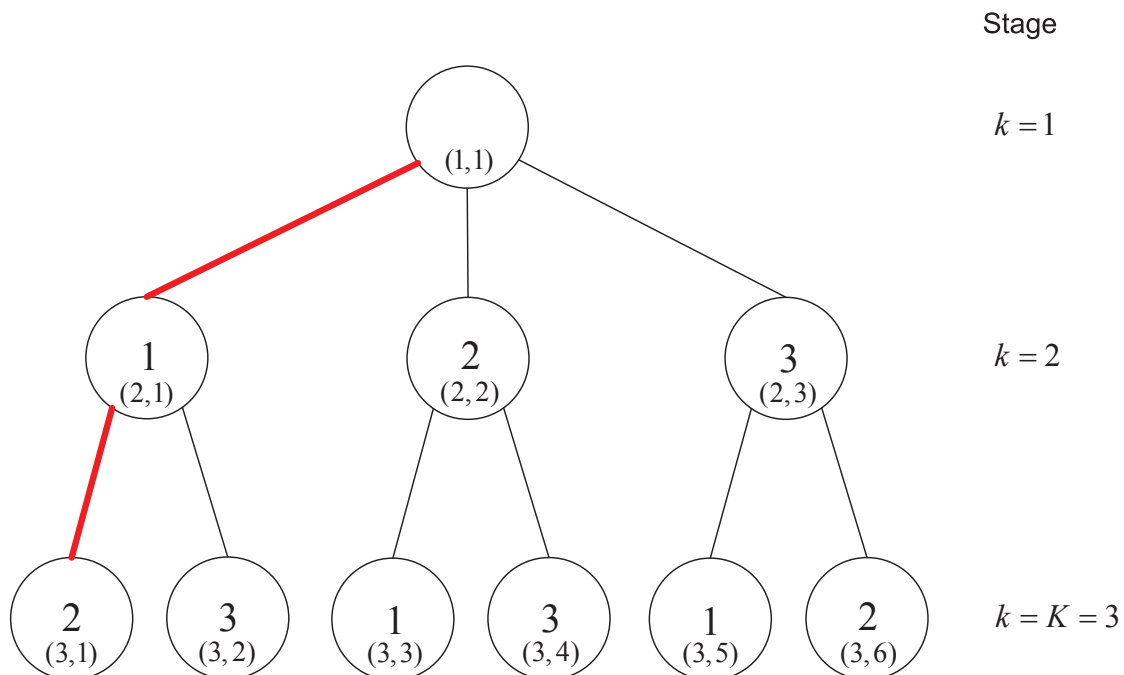


Fig. 2. The multiuser decoding tree for the K -stage coset decoding in Table II with $K = 3$. Here for each node, the label (k, j) denotes the j -th node from the left at the k -th stage (Node_stage in Table II), while the number i inside a circle denotes the index i of the user assumed to have been correctly decoded at the previous stage (Node_user in Table II). For example, when the coset decoding in Table II is performed at node $(2, 1)$ (the leftmost child node of the root node), user 1 is assumed to have been correctly decoded. The path from root node $(1, 1)$ to node $(3, 1)$ is illustrated with bolder lines.

2) *K -stage coset decoder*: We first introduce the decoder at the destination, which generalizes the single stage coset decoder in [10] to the multi-stage one. The coset decoder disregards the boundaries of the codewords and avoids the complicated boundary control [12], which allows for significant complexity reductions compared to ML decoding. Moreover, it facilitates the efficient sphere decoding algorithm [11], [12]. To decode messages from the received signal \mathbf{y}_{dst} in (6), the proposed K -stage coset decoder works as in Table II with the detailed steps explained as follows.

According to Table II, the decoder first generates the decoding tree as in Step A. An example for $K = 3$ is given in Fig. 2. The decoder will traverse nodes from stage 1 to K in the tree, and produce the candidate codewords. We take the root node in Fig. 2 as an example to explain Steps B.1 and B.2 in Table II. We use the notation $\bar{\mathbf{c}}(\mathbf{w}_t)$ to represent the super-codeword for the $K + 1$ transmitters corresponding to the

TABLE II
ALGORITHM OF THE K -STAGE COSET DECODING FOR THE DESTINATION*

A. Generation of the decoding tree:

Initialization: For the root node, Node_user= empty, Node_stage= 1
for $k = 1 : K - 1$
 for each node with node_stage= k ,
 generates $(K - k + 1)$ child nodes for the next stage (Node_stage= $k + 1$),
 for the child nodes from left to right,
 Node_user are assigned from the set $\{1, \dots, K\} \setminus \mathcal{S}$ in increasing order,
 where $\mathcal{S} = \{j : \text{Node_user} = j, \text{for the ancestors}^{**} \text{ of child node}\}$

end

B. K -stage candidate generation via coset decoding:

for $k = 1 : K$

Step B.1: For the node (k, j) , let $\mathbf{y}_{dst}^{(k,j)} = \mathbf{y}_{dst} - \sum_{i \in \mathcal{S}_p^{(k,j)}} \mathbf{H}_i^d \hat{\mathbf{x}}_i$, where $\mathcal{S}_p^{(k,j)}$ is the set of previously-decoded users i along the path from root node to node (k, j) , $\hat{\mathbf{x}}_i$ is the transmitted signal (from (10)) corresponding to previous-decoded user i 's message, and the channel \mathbf{H}_i^d is formed from (8).

(For example, for the path starting from root node to node (3,1) in Fig. 2, the set $\mathcal{S}_p^{(3,1)}$ is $\{1, 2\}$.)

Step B.2: Decodes the users' messages in the residual user set $\mathcal{S}^{(k,j)} = \{1, \dots, K\} \setminus \mathcal{S}_p^{(k,j)}$ by coset decoding

$$\hat{\mathbf{c}}^{(k,j)} = \arg \min_{\mathbf{c} \in \mathcal{O}^\Psi, (k,j)} \mathbf{M}^{(k,j)}(\mathbf{c}^{(k,j)}),$$

where

$$\mathbf{M}^{(k,j)}(\mathbf{c}^{(k,j)}) = \left| \mathbf{F}_{dst}^{(k,j)} \mathbf{y}_{dst}^{(k,j)} + \mathbf{B}_{dst}^{(k,j)} (\mathbf{u}^{(k,j)} - \mathbf{c}^{(k,j)}) \right|^2. \quad (\text{T2.1})$$

Let $m_k = 2((K - k + 1)M_u + M_r)LT$ and $N' = 2NLT$, the $m_k \times 1$ $\mathbf{c}^{(k,j)}$ is formed from the super-codeword \mathbf{c} by collecting all $\mathbf{c}_i \in \Lambda_{C_i}$ of transmitter i ((T1.4) in Table I) where $i \in \{\mathcal{S}^{(k,j)}, K + 1\}$; the dither signal $\mathbf{u}^{(k,j)}$ is formed from \mathbf{u} similarly; the $m_k \times N'$ $\mathbf{F}_{dst}^{(k,j)}$ and $m_k \times m_k$ $\mathbf{B}_{dst}^{(k,j)}$ are the corresponding MMSE -GDFE filters for $\mathbf{c}^{(k,j)}$; and the searching cosets formed by previously-decoded users $i \in \mathcal{S}_p^{(k,j)}$ is

$$\mathcal{O}^{\Psi, (k,j)} = \{\mathbf{c} : \mathbf{c} \in \mathcal{O}^\Psi, (\mathbf{c}_i \bmod \Lambda_{S_i}) = (\hat{\mathbf{c}}_i^{p, (k,j)} \bmod \Lambda_{S_i}), i \in \mathcal{S}_p^{(k,j)}\},$$

where \mathcal{O}^Ψ is given in (12), $\mathbf{c}_i \in \Lambda_{C_i}$ ((T1.4) in Table I) where Λ_{C_i} is transmitter i 's coding lattice, and $(\hat{\mathbf{c}}_i^{p, (k,j)} \bmod \Lambda_{S_i})$ is the codeword (coset leader) of the previously-decoded user i where $i \in \mathcal{S}_p^{(k,j)}$.

end

C. Candidate elimination:

For node (K, j) at the final stage K , combine the decoded messages to produce the $K \times 1$ super-message $\hat{\mathbf{w}}_t^{(K,j)}$ as the candidate at node (K, j) . The decoder searches for all $K!$ candidates $\hat{\mathbf{w}}_t^{(K,j)}$ and declares the one such that $\mathbf{H}_{dst} \hat{\mathbf{x}}^{(K,j)}$ is nearest to the received signal \mathbf{y}_{dst} as the final decoded message, where $\hat{\mathbf{x}}^{(K,j)}$ is the transmitted signal according to message $\hat{\mathbf{w}}_t^{(K,j)}$.

* The algorithm for the relay can be identically obtained by ignoring the relay's codewords.

** The ancestors of a node are all the nodes along the path from the root to that node (not included).

$K \times 1$ transmitted message vector $\mathbf{w}_t = [(\mathbf{w}_t)_1, \dots, (\mathbf{w}_t)_K]^T$, where $(\mathbf{w}_t)_i$ denotes the transmitted message for user i . For the root node (the first stage coset decoding), with received signal \mathbf{y}_{dst} at the destination; the decoder output $\hat{\mathbf{c}}$ according to (10) is

$$\hat{\mathbf{c}} = \arg \min_{\mathbf{c} \in \mathcal{O}^\Psi} \mathbf{M}(\mathbf{c}), \quad \text{with } \mathbf{M}(\mathbf{c}) = |\mathbf{F}_{dst} \mathbf{y}_{dst} + \mathbf{B}_{dst} (\mathbf{u} - \mathbf{c})|^2, \quad (11)$$

where \mathbf{F}_{dst} and \mathbf{B}_{dst} are the forward and feedback filters of the minimum mean-square error (MMSE) estimation generalized decision feedback equalizer (GDFE) as defined in [10] and [16] respectively; $\mathbf{u} = [\mathbf{u}_1^T, \dots, \mathbf{u}_{K+1}^T]^T$ and the decoder searches points in the cosets \mathcal{O}^Ψ (see (12)) of all $\bar{\mathbf{c}}(\mathbf{w})$ (defined similarly to $\bar{\mathbf{c}}(\mathbf{w}_t)$ above), $\mathbf{w} \in \mathcal{W}$, with \mathcal{W} being the set of all possible messages:

$$\mathcal{O}^\Psi \triangleq \{\mathbf{c} \in \Lambda_{C_{ur}} : (\mathbf{c} \bmod \Lambda_{S_{ur}}) = \bar{\mathbf{c}}(\mathbf{w}), \mathbf{w} \in \mathcal{W}\}, \quad (12)$$

where the super-lattice of users and the relay $\Lambda_{C_{ur}}$ is defined in (T1.9) of Table I. The decoded message $\hat{\mathbf{w}}_t$ is declared if $\bar{\mathbf{c}}(\hat{\mathbf{w}}_t)$ and the decoded $\hat{\mathbf{c}}$ from (11) belong to the same coset, $\hat{\mathbf{c}} \bmod \Lambda_{S_{ur}} = \bar{\mathbf{c}}(\hat{\mathbf{w}}_t)$. For the node (k, j) in the decoding tree (the j -th node from the left at k -th stage) we consider a path from the root node to node (k, j) . An example for $(k, j) = (3, 1)$ is given in Fig. 2. In Step B.1 of Table II, the decoder assumes that all the users at the nodes along the path (users 1 and 2 for the example path in Fig. 2), have already been successively decoded (not necessarily correctly), and subtract the corresponding transmitted signals from the received signal \mathbf{y}_{dst} . Then the decoder decodes the remaining transmitted messages by (T2.1) in the Step B.2 of Table II (which corresponds to (11)). Finally, as in Step C, the decoder searches for all $K!$ candidates produced at the nodes at the K -th stage (instead of all $2^{LT \sum_{i=1}^K R_i}$ codewords) to choose the final decoded message.

The decoder at the relay also uses (11) as the criterion to decode messages from \mathbf{y}_{relay} in (5) with the corresponding MMSE-GDFE forward and feedback filters. The main difference is that now the decoding does not make use of the relay codebook, and the decoder searches in the super-lattice of users Λ_{C_u} instead of the coset \mathcal{O}^Ψ in (12). The complexity of the decoder in Table II is about $\left(\sum_{k=1}^K \frac{K!}{(K-k+1)!} O(m_k^3) + K! O(m_K^2) \right) = O((LT)^3)^\ddagger$, where $m_k = 2((K-k+1)M_u + M_r)LT$. It is much smaller compared with the complexity of the ML decoder $O(2^{LT \sum_{i=1}^K R_i})$, which grows exponentially with the block length LT .

[‡] According to our practical design in Section V, one can use a linear mapper to implement O-MLC and MS-MLC. Then the m_k -dimensional coset decoder can be implemented by the sphere decoding algorithm in [12] with complexity roughly being $O(m_k^3)$.

Note that since the super-codewords have to satisfy the relay mapping rule (which may not be linear) in Section III-B, the set \mathbb{O}^Ψ is *not* necessary a sublattice of $\Lambda_{C_{ur}}$. This makes (11) different from the MMSE-GDFE *lattice* decoder in [10] and [16]. Without the algebraic structure of a lattice, the upcoming error probability analysis in the next section, and the design of practical decoding algorithms for the simulations in Section V will be much more difficult than those in [10].

IV. PERFORMANCE ANALYSIS OF THE PROPOSED CODING SCHEMES

In this section, we establish the achievable rate regions for the MARC defined in (5) and (6), using the proposed O-MLC and MS-MLC for a fixed channel matrix, respectively. We show that the rate performance, which was originally achieved by using an unstructured random codebook in [7], is now achieved by our structured O-MLC. The key is using the K -stage coset decoder which performs successive cancellation on the multiuser decoding tree, thus avoiding the rate loss incurred by the one-stage coset decoder in [10]. The rate loss due to use of a one-stage coset decoder is derived in Corollary 1. However, in Corollary 2, we show that the rate loss is relatively small in the high SNR regime, and structured O-MLC with the one-stage coset decoder achieves the optimal DMT for the MARC in (5) and (6). Note that the DMT was achieved by an unstructured random codebook and ML decoding in [8]. For MS-MLC, we show that it can approach the rate performance of O-MLC by increasing the relay's codebook size, and thus can tradeoff between the rate performance and complexity.

In the error analysis of the proposed schemes, the conventional approach tailored for ML decoding [5] [8] and [20] fails in predicting the performance of the coset decoder in (11) due to the infinite number of points $\mathbf{c} \in \mathbb{O}^\Psi$ where the set \mathbb{O}^Ψ is defined in (12). To solve this problem, from (12), we define the *differential ambiguity cosets* for the event that the transmitted message \mathbf{w}_t is erroneously decoded as \mathbf{w} as

$$\mathbb{O}^{\Psi\Delta} \triangleq \{\mathbf{d} \in \Lambda_{C_{ur}} : \bar{\mathbf{d}} = \bar{\mathbf{d}}(\mathbf{w}), \mathbf{w} \in \mathcal{W}, \mathbf{w} \neq \mathbf{w}_t\}, \quad (13)$$

where the *differential codeword* $\bar{\mathbf{d}}(\mathbf{w}) \triangleq (\bar{\mathbf{c}}(\mathbf{w}) - \bar{\mathbf{c}}(\mathbf{w}_t)) \bmod \Lambda_{S_{ur}}$ with $\Lambda_{S_{ur}}$ given in (T1.9) of Table I and the vector after modulo operation $\bar{\mathbf{d}}$ is defined in (T1.10). From the closure property of lattice addition, $\bar{\mathbf{d}}(\mathbf{w}) \in \Lambda_{C_{ur}}$. Moreover, $\mathbb{O}^{\Psi\Delta}$ is not a direct product of $K+1$ lattices (i.e., $\Lambda_{C_{ur}}$), and thus the techniques in [10] fail to predict the error probability of O-MLC. We propose a new error probability upper-bound which avoids directly counting points of $\mathbb{O}^{\Psi\Delta}$ in the decision region of the decoder as this kind of evaluation is

intractable. Please see the upcoming Lemma 1 presented in the proof of Theorem 1 and the discussions after it.

Besides providing the aforementioned new proof techniques, we also show that there will be a rate loss due to the one-stage coset decoding in [10]. The loss can be circumvented with the proposed K -stage coset decoders by letting the decoder successively cancel the previously decoded messages. We show that in our multiuser decoding tree as in Fig. 2, there exists at least one path at each stage of Step B of Table II on which the previously decoded messages are correct. Then we can *at least* obtain a better decoder for the remaining users in the next stage to improve the error performance. To show that we can always choose the correct codeword from the candidates at the final stage in the decoding tree, we use a suboptimal decoder instead of the optimal one in Step C of Table II to complete our proof. Note that our decoder is different from the successive MAC decoding studied in [21], where the decoder is based on ML decoding and the previously decoded messages are correct.

Now, we are ready to derive the achievable rate region of (5) and (6), using O-MLC as follows.

Theorem 1: For the MARC in (5) and (6), the DDF rate region in (14) and (15), which is achieved by unstructured Gaussian codebooks and ML decoding in [7], is achievable by the *structured* O-MLC and the K -stage coset decoder in Table II, where the rate constraints at the relay and destination are

$$\sum_{i \in S} R_i < \frac{1}{LT} R_{unG}^{relay}(\mathbf{H}_{relay}^S), \text{ and} \quad (14)$$

$$\sum_{i \in S} R_i < \frac{1}{LT} R_{unG}^{dst}(\mathbf{H}_{dst}^{\{S, K+1\}}), \quad \forall S \subseteq \{1, \dots, K\} \quad (15)$$

respectively, with $R_{unG}^{dst}(\mathbf{H}_{dst}^{\{S, K+1\}})$ and $R_{unG}^{relay}(\mathbf{H}_{relay}^S)$ given in (T1.18) and (T1.19) in Table I. The channel matrix from the users in the set S and the relay to the destination $\mathbf{H}_{dst}^{\{S, K+1\}}$ is formed from $\mathbf{H}_{dst} = [\mathbf{H}_1^d, \dots, \mathbf{H}_{K+1}^d]$ as in (T1.17) with \mathbf{H}_i^d given in (8) and (9), and the channel matrix from the users in the set S to the relay \mathbf{H}_{relay}^S is defined similarly to $\mathbf{H}_{dst}^{\{S, K+1\}}$.

Proof: We prove only (15) here since (14) follows similarly. First, for the first stage ($k = 1$, the root node of Fig. 2) of the candidate generation process in Step B of Table II, we show that at least one of the users' messages is correctly decoded in the generated "super"-message $\hat{\mathbf{w}}_t^{(1,1)}$ of all users (with probability 1) as $T \rightarrow \infty$. To do this, we first define the following error event.

Definition 4 (set-S error): A decoded super-message \mathbf{w} is with set-S error if the message in \mathbf{w} for every

user i , where $i \in S$, is different from the corresponding transmitted message. That is, $\mathbf{w}_i \neq (\mathbf{w}_t)_i, \forall i \in S$, while $\mathbf{w}_i = (\mathbf{w}_t)_i$, otherwise.

Let $P_e(S|\mathbf{H}_{dst})$ be the probability that there exists \mathbf{w} with set- S error with fixed \mathbf{H}_{dst} , and $\min_{\mathbf{c} \in \mathbf{o}(\mathbf{w})} M(\mathbf{c}) \leq \min_{\mathbf{c} \in \mathbf{o}(\mathbf{w}_t)} M(\mathbf{c})$, with $M(\mathbf{c})$ defined in (11) and $\mathbf{o}(\mathbf{w})$ being the coset of \mathbf{w} . To validate our claim, we first consider the erroneous user set $\mathcal{S}^{(1)} = \{1, \dots, K\}$ and will prove that $P_e(\mathcal{S}^{(1)}|\mathbf{H}_{dst}) \rightarrow 0$ for the first-stage, if the transmission rates R_i satisfy (15) and the lattice codes are good as defined in the upcoming Lemma 1. Here $P_e(\mathcal{S}^{(1)}|\mathbf{H}_{dst})$ is averaged over the random relay-mapper and linear-code ensemble $\mathcal{E}_{\Psi, C^{Lo}} = \{\Psi^{one}, C_{ur}^{Lo}\}$ consisting of all possible one-to-one mappers Ψ^{one} and Loeliger linear codes C_{ur}^{Lo} of the users and relay ((T1.6) in Table I).

Lemma 1: For O-MLC, let $R_i, i = 1, \dots, K+1$, be the code rates for the users and the relay, and $\{\Lambda_{C_i}\}$ belong to the Loeliger lattices ensembles (cf. Definition 5 in Appendix A-(I)). For stage $k = 1$ of Step B in Table II, as $LT \rightarrow \infty$, the set- $\mathcal{S}^{(1)}$ error probability (cf. Definition 4), where $\mathcal{S}^{(1)} = \{1, \dots, K\}$, satisfies

$$\begin{aligned} P_e(\mathcal{S}^{(1)}|\mathbf{H}_{dst}) &\leq \frac{1}{|\mathcal{E}_{\Psi, C^{Lo}}|} \sum_{(\Psi^{one}, C_{ur}^{Lo}) \in \mathcal{E}_{\Psi, C^{Lo}}} \left| \mathbb{O}_{\mathcal{S}^{(1)}}^{\Psi_{\Delta}^{one}} \cap \mathcal{R}_{\beta} \right| \\ &\leq \exp \left(\frac{-LT}{\log e} \left[\frac{1}{LT} R_{unG}^{dst}(\mathbf{H}_{dst}^{\{\mathcal{S}^{(1)}, K+1\}}) - \sum_{i \in \mathcal{S}^{(1)}} R_i + \frac{1}{LT} \log \frac{2^{R_{K+1}LT} - 1}{2^{R_{K+1}LT}} \right] \right) \end{aligned} \quad (16)$$

where $\mathbb{O}_{\mathcal{S}^{(1)}}^{\Psi_{\Delta}^{one}}$ consists of points belonging to the differential ambiguity cosets for O-MLC $\mathbb{O}_{\mathcal{S}^{(1)}}^{\Psi_{\Delta}^{one}}$ (cf. (13)), with corresponding messages having set- $\mathcal{S}^{(1)}$ errors; $\mathcal{E}_{\Psi, C^{Lo}} = \{\Psi^{one}, C_{ur}^{Lo}\}$ is defined right before Lemma 1; the decision region $\mathcal{R}_{\beta} \triangleq \{\mathbf{v} : |\mathbf{B}_{dst} \mathbf{v}|^2 \leq (KM_u + M_r)LT(1 + \beta)\}$ with filter \mathbf{B}_{dst} defined as in (11) and $\beta > 0$; and the rate constraint $R_{unG}^{dst}(\mathbf{H}_{dst}^{\{\mathcal{S}^{(1)}, K+1\}})$ is defined as in (15).

The proof of Lemma 1 is given in Appendix A. The main difficulty is that the cosets $\mathbb{O}_{\mathcal{S}^{(1)}}^{\Psi_{\Delta}^{one}}$ is not a direct product of $K+1$ lattices as in [10], so the methods in [10] and [17] *cannot* be directly applied to counting the number of points of $\mathbb{O}_{\mathcal{S}^{(1)}}^{\Psi_{\Delta}^{one}}$ in the decision region \mathcal{R}_{β} in the second inequality of (16). We avoid explicitly counting points in $\mathbb{O}_{\mathcal{S}^{(1)}}^{\Psi_{\Delta}^{one}}$ by developing new upper-bounds as in (26) and (27) in Appendix A. Otherwise, naively applying the methods of [10] and [17] will result in rates as in (16) but without the factor $(2^{R_{K+1}LT} - 1)$ cancelling out $2^{R_{K+1}LT}$, and lead to significant rate loss compared with our (15) with $S = \mathcal{S}^{(1)}$ since $R_{K+1} = \sum_{i=1}^K R_i$ is required to ensure the one-to-one mapping.

With the results for the first stage $k = 1$ in Lemma 1, we show by induction that after the candidate generation process in Step B of Table II, among all ‘‘super’’-message $\hat{\mathbf{w}}_t^{(K,j)}$ at stage K (defined in Step C),

there exists a correct one almost surely (with probability 1) as $T \rightarrow \infty$. To do this, we will show that for stage k , with at least $k - 1$ (almost surely) correctly decoded users from the previous stage, almost surely there exists one node (k, j'_k) having at least k users correctly decoded. Note that for stage k , conditioned on the event that all decoded users' messages from the previous stages are correct, the noise \mathbf{n}_{dst} in (6) may *no longer* be Gaussian [21]. However, under the condition (15), the probability $P_e^{(k)}$ that there exists no node at stage k having at least k users correctly decoded can be shown to still satisfy

$$P_e^{(k)} \stackrel{(a)}{\leq} P_e(\mathcal{S}^{(1)} | \mathbf{H}_{dst}) + \sum_{s=2}^k P_e^G(\mathcal{S}^{(s, j'_s)} | \mathbf{H}_{dst}, \mathcal{S}_p^{(s, j'_s)}) \stackrel{(b)}{\rightarrow} 0, \quad (17)$$

as $LT \rightarrow \infty$, where $P_e^G(\mathcal{S}^{(s, j'_s)} | \mathbf{H}_{dst}, \mathcal{S}_p^{(s, j'_s)})$ is defined under Gaussian \mathbf{n}_{dst} and will be given below and (17 a) follows from [21]. Then our claim for stage K is valid and $P_e^{(K)} \rightarrow 0$ by induction. Since under (15), as $LT \rightarrow \infty$, $P_e(\mathcal{S}^{(1)} | \mathbf{H}_{dst}) \rightarrow 0$ from (16), we will show that $P_e^G(\mathcal{S}^{(s, j'_s)} | \mathbf{H}_{dst}, \mathcal{S}_p^{(s, j'_s)}) \rightarrow 0, \forall s \leq k$, in this setting to validate (17 b). Now we introduce the definition of $P_e^G(\mathcal{S}^{(s, j'_s)} | \mathbf{H}_{dst}, \mathcal{S}_p^{(s, j'_s)})$ as follows. Let $\mathcal{S}_p^{(s, j'_s)}$ be the set of $s - 1$ previous users along the path starting from the root node to node (s, j'_s) , the j'_s -th node at stage s , in the decoding tree shown in Fig. 2. Also, let the set $\mathcal{S}^{(s, j'_s)}$ be $\{1, \dots, K\} \setminus \mathcal{S}_p^{(s, j'_s)}$. Then $P_e^G(\mathcal{S}^{(s, j'_s)} | \mathbf{H}_{dst}, \mathcal{S}_p^{(s, j'_s)})$ is defined as the probability that there exists \mathbf{w} with set- $\mathcal{S}^{(s, j'_s)}$ error (Definition 4) conditioned on the event that all users in $\mathcal{S}_p^{(s, j'_s)}$ are correct (the existence of j'_s is guaranteed by the assumption of induction $P_e^{(s-1)} \rightarrow 0, 1 < s \leq k$), and \mathbf{n}_{dst} in (6) is conditionally Gaussian. For this kind of error events, $\min_{\mathbf{c} \in \mathbf{o}(\mathbf{w})} \mathbf{M}^{(s, j'_s)}(\mathbf{c}) \leq \min_{\mathbf{c} \in \mathbf{o}(\mathbf{w}_t)} \mathbf{M}^{(s, j'_s)}(\mathbf{c})$ with $\mathbf{M}^{(s, j'_s)}(\mathbf{c})$ defined on the right-hand side (RHS) of (T2.1) in Table II. As in the proof for Lemma 1 in Appendix A, we can similarly upper-bound $P_e^G(\mathcal{S}^{(s, j'_s)} | \mathbf{H}_{dst}, \mathcal{S}_p^{(s, j'_s)})$ by the RHS of (16) with $\mathcal{S}^{(1)}$ replaced by $\mathcal{S}^{(s, j'_s)}$. Thus if the transmission rates R_i satisfy (15), as $T \rightarrow \infty$, we have that $P_e^G(\mathcal{S}^{(s, j'_s)} | \mathbf{H}_{dst}, \mathcal{S}_p^{(s, j'_s)}) \rightarrow 0$, which verifies (17 b). This validates our claim for stage K .

For the Step C of Table II, we will use the following suboptimal decoder instead of the optimal decoder in Table II to prove that we can find the correct message \mathbf{w}_t almost surely. First, we compare candidates $\hat{\mathbf{w}}_t^{(K,1)}$ and $\hat{\mathbf{w}}_t^{(K,2)}$, and form the set of users \mathcal{S}_c so that for any $i \in \mathcal{S}_c$, $\hat{\mathbf{w}}_t^{(K,1)}$ and $\hat{\mathbf{w}}_t^{(K,2)}$ have a common message for user i . Then we compare the ‘‘coset’’-distances $\min_{\mathbf{c} \in \mathbf{o}(\hat{\mathbf{w}}_t^{(K,1)})} \mathbf{D}^{(k_c)}(\mathbf{c})$ and $\min_{\mathbf{c} \in \mathbf{o}(\hat{\mathbf{w}}_t^{(K,2)})} \mathbf{D}^{(k_c)}(\mathbf{c})$ of these two candidates and choose the one with smaller ‘‘coset’’-distance (if equal, we randomly select one), where $\mathbf{D}^{(k_c)}(\mathbf{c})$ is formed by replacing $\mathcal{S}_p^{(k, j)}$ with \mathcal{S}_c in $\mathbf{M}^{(k, j)}(\mathbf{c})$ in (T2.1) of Table II (also the corresponding parameters). We then compare the chosen candidate with the next candidate

$\hat{\mathbf{w}}_t^{(K,3)}$, and so on. After $K! - 1$ comparisons among total $K!$ candidates, the final chosen candidate in the final comparison will be declared as the decoded message. Now we show that the error probability of the above sub-optimal decoder will approach zero. As in (17 a), this error probability is upper-bounded by $P_e^{(K)} + P_e^G(\hat{\mathbf{w}}_t^{(K,j)} | \hat{\mathbf{w}}_t^{(K,j'_K)} = \mathbf{w}_t)$, where $P_e^{(K)}$ is defined before (17) and $P_e^G(\hat{\mathbf{w}}_t^{(K,j)} | \hat{\mathbf{w}}_t^{(K,j'_K)} = \mathbf{w}_t)$ is the probability that the sub-optimal decoder outputs incorrect $\hat{\mathbf{w}}_t^{(K,j)} \neq \mathbf{w}_t$ conditioned on the event that there is one correct candidate $\hat{\mathbf{w}}_t^{(K,j'_K)} = \mathbf{w}_t$ and the noise \mathbf{n}_{dst} is Gaussian. Since $P_e^{(K)} \rightarrow 0$ according to the previous paragraph, we will show $P_e(\hat{\mathbf{w}}_t^{(K,j)} | \hat{\mathbf{w}}_t^{(K,j'_K)} = \mathbf{w}_t) \rightarrow 0$ and then our proof is complete. Specifically, if the decoder output $\hat{\mathbf{w}}_t^{(K,j)} \neq \mathbf{w}_t$, it will have smaller (or equal) ‘‘coset’’-distance than that of $\hat{\mathbf{w}}_t^{(K,j'_K)} = \mathbf{w}_t$, i.e., $\min_{\mathbf{c} \in \mathbf{o}(\hat{\mathbf{w}}_t^{(K,j)})} \mathbf{D}^{(k_c)}(\mathbf{c}) \leq \min_{\mathbf{c} \in \mathbf{o}(\hat{\mathbf{w}}_t^{(K,j'_K)})} \mathbf{D}^{(k_c)}(\mathbf{c})$, and now \mathcal{S}_c becomes the set of correctly decoded users in $\hat{\mathbf{w}}_t^{(K,j)}$ since it is the set of users with common messages for both $\hat{\mathbf{w}}_t^{(K,j)}$ and the correct $\hat{\mathbf{w}}_t^{(K,j'_K)} = \mathbf{w}_t$. That is, message $\hat{\mathbf{w}}_t^{(K,j)}$ may have $\text{set}-(\mathcal{S}_c)^c$ error (Definition 4) given that the users in \mathcal{S}_c are correct, where $(\mathcal{S}_c)^c = \{1, \dots, K\} \setminus \mathcal{S}_c$. However, from the derivations in the previous paragraph, conditioned on the event that users in \mathcal{S}_c are correct, the probability of $\text{set}-(\mathcal{S}_c)^c$ error $P_e^G((\mathcal{S}_c)^c | \mathbf{H}_{dst}, \mathcal{S}_c) \rightarrow 0$. This is a contradiction and $P_e^G(\hat{\mathbf{w}}_t^{(K,j)} | \hat{\mathbf{w}}_t^{(K,j'_K)} = \mathbf{w}_t) \rightarrow 0$. Thus our suboptimal decoder will always find the correct \mathbf{w}_t , and this concludes our proof since the optimal decoder in Table II will perform even better. ■

If only the one-stage coset decoder is used as in [10], we have the following.

Corollary 1: For the MARC in (5) and (6), the rate region constrained by (18) and (19), which is strictly smaller than that in Theorem 1, is achievable by O-MLC with the one-stage coset decoder in (11), where

$$\sum_{i \in \mathcal{S}} R_i < \frac{1}{LT} R_{unG}^{relay}(\mathbf{H}_{relay}^{\mathcal{S}}) - M_u |S| \log \frac{K}{|S|} \quad \text{and}, \quad (18)$$

$$\sum_{i \in \mathcal{S}} R_i < \frac{1}{LT} R_{unG}^{dst}(\mathbf{H}_{dst}^{\{\mathcal{S}, K+1\}}) - (M_u |S| + M_r) \log \frac{KM_u + M_r}{|S|M_u + M_r}, \quad \forall \mathcal{S} \subseteq \{1, \dots, K\}. \quad (19)$$

The proof can be easily obtained by modifying Lemma 1, in which we count all of the points in cosets $\mathcal{O}_{\Delta}^{one}$ instead of only counting those corresponding to the message with $\text{set}-\mathcal{S}^{(1)}$ error (Definition 4) as in $\mathcal{O}_{\mathcal{S}^{(1)}}^{\Delta, one}$ of (16), and follows arguments similar to those used in Theorem 1. The details are omitted here. Clearly, compared to the rate region in (14) and (15), there are rate loss terms $M_u |S| \log \frac{K}{|S|}$ and $(M_u |S| + M_r) \log \frac{KM_u + M_r}{|S|M_u + M_r}$ in (18) and (19), respectively. These losses are zero when $|S| = K$, and the MMSE-GDFE processing for the one-stage coset decoding in (11) is only sum rate optimal.

For MS-MLC, we have the following theorem. In this result, in addition to the same rate constraints (14) and (15) as in Theorem 1, there is an additional rate constraint (20) for MS-MLC which makes the achievable rate region smaller than that for O-MLC.

Theorem 2: For the MARC in (5) and (6), using MS-MLC and the K -stage coset decoder in Table II, the rate region with constraints in (14) and (15) and the following additional constraint (20) is achievable, where

$$\sum_{i \in S} R_i < \frac{1}{LT} R_{unG}^{dst}(\mathbf{H}_{dst}^S) - M_u |S| \log \frac{|S| M_u + M_r}{|S| M_u} + R_{K+1} \quad \forall S \subseteq \{1, \dots, K\}, |S| > 1. \quad (20)$$

When using MS-MLC with one-stage coset decoder in (11), the rate region with the constraints in (18) and (19) and the following additional constraint (21) is achievable, where

$$\sum_{i \in S} R_i < \frac{1}{LT} R_{unG}^{dst}(\mathbf{H}_{dst}^S) - M_u |S| \log \frac{KM_u + M_r}{|S| M_u} + R_{K+1} \quad \forall S \subseteq \{1, \dots, K\}, |S| > 1. \quad (21)$$

Proof: Unlike O-MLC, there is a possibility for MS-MLC that two different users' super-codewords are mapped to the same relay codeword from Definition 3. This fact makes the properties exploited in Lemma 1 for the random mapped-codebook ensemble of O-MLC (for details, please see the proof of (28) in Appendix A) no longer hold for the ensemble for MS-MLC. Thus Lemma 1 cannot be applied for MS-MLC. We solve this problem by dividing the random mapped-codebook ensemble for MS-MLC into two partitions, and the techniques for proving Lemma 1 can be modified to deal with each partition separately. The detailed proof is given in Appendix B. The rate region for one-stage coset decoder in (18), (19) and (21) follows by using techniques similar to those used in the proof of Corollary 1. ■

The additional rate constraint (20) is due to the ambiguity of the modulo-sum mapper in MS-MLC, where there is a rate loss term $M_u |S| \log \frac{|S| M_u + M_r}{|S| M_u}$. However, the rate constraint (20) can be negligible and even looser than constraint (15), as $(R_{K+1} - M_u |S| \log \frac{|S| M_u + M_r}{|S| M_u})$ becomes larger by increasing the relay codebook size $2^{R_{K+1} LT}$ (which reduces the occurrence of ambiguity). Thus MS-MLC can approach the performance of O-MLC by increasing the complexity.

Finally, for random slow fading channels, we show that O-MLC with the one-stage coset decoder (11) is DMT optimal for the DDF MARC, as stated in the following corollary. Despite the rate loss terms in (18) and (19) compared with (14) and (15), respectively, the losses become relatively negligible for the DMT analysis when the SNR is high.

Corollary 2: For the MARC in (5) and (6), with the one-stage coset decoder (11), the O-MLC achieves the optimal DDF DMT $d(\mathbf{r})$ of (5) and (6), respectively, where $d(\mathbf{r})$ is defined in (T1.20) of Table I.

Sketch of proof: As in [3] and [8], we need to establish the DMT optimality for both the relay and destination channels. We focus on the destination channel (6) since the DMT-optimality for the relay channel (5) (identical to the MAC channel) has been proved in [10]. Following [16] and the proof steps for (19), we can exponentially upper-bound the error probability $P_e(\rho_d)$ in (T1.20) of Table I using decoder (11) (averaged over random \mathbf{H}_{dst} which satisfy (15)) as

$$P_e(\rho_d) \stackrel{\leq}{\leq} E_{\mathbf{H}_{dst}} \left[(1 + \delta) \cdot \sum_{S \subseteq \{1, \dots, K\}, S \neq \emptyset} \rho_d^{LT \sum_{i \in S} r_i} \exp \left[\frac{-1}{\log e} R_{unG}^{dst} \left(\mathbf{H}_{dst}^{\{S, K+1\}} \right) \right] \right] \doteq Pr(O) \quad (22)$$

where $\delta > 0$, ρ_d is the received SNR at the destination; r_i is the given multiplexing gain for user i as in (T1.20); the exponential larger and equal [20] are denoted as $\stackrel{\leq}{\leq}$ and \doteq ; and O is the outage event when \mathbf{H}_{dst} does not satisfy (15). The proof of (22) is detailed in Appendix D. Together with the fact that for any coding schemes, $P_e(\rho_d) \stackrel{\geq}{\geq} Pr(O) \doteq \rho_d^{-d(\mathbf{r})}$ as in [20], we prove that O-MLC can achieve the optimal DMT $d(\mathbf{r})$ for the destination. ■

In [8], a two-user, single antenna node MARC was studied for the symmetric rate case ($R_1 = R_2$), which showed that the DDF strategy achieves the optimal DMT for the MARC in the low to medium multiplexing gain regime. The DMT results of Corollary 2 can be achieved by codebooks, which are more structured than that in [8]. Moreover, our designs in the next section also demonstrate that our theoretical results can be implemented in practice.

V. SIMULATION RESULTS

In this section, we present numerical examples to illustrate our theoretical results. Performance results based on practical decoders are also presented. As mentioned in Section III-C, the *lattice decoder* in [10] and [16] fails to be directly applicable to our *coset decoder* of (11) since only the points in \mathcal{O}^Ψ of (12) will be searched. In general, the optimal non-linear relay mapper may make the coset decoders very complicated and impractical. To facilitate the coset decoder for the relay mapper, we resort to the sub-optimal *linear* mapper such that the coset decoder of (11) can be transformed into the efficient lattice decoder. For simplicity, we consider the case in which there are two users with the same transmission rate, i.e., $R_1 = R_2 = R$.

Let the code rate of the relay $R_3 = 2R$, and \mathbf{G}_i , $i = 1, 2, 3$, be the generation matrix of the coding lattice Λ_{C_i} (cf. Definition 5) for transmitter i . Then for user $i = 1, 2$, the codewords are $\bar{\mathbf{c}}_i = (\mathbf{G}_i \tilde{\mathbf{z}}_i \bmod \Lambda_{S_i})$, where $\tilde{\mathbf{z}}_i \in \mathbb{Z}^{2M_u LT}$. For O-MLC, with $M_r = 2M_u$, we choose the linear relay mapping such that the relay codewords are $\bar{\mathbf{c}}_3 = (\mathbf{G}_3 \tilde{\mathbf{z}}_3 \bmod \Lambda_{S_3})$ with $\tilde{\mathbf{z}}_3 = [\tilde{\mathbf{z}}_1^T, \tilde{\mathbf{z}}_2^T]^T$. After some manipulations, it can be verified that the decoding equation of (11) is transformed into

$$\hat{\mathbf{z}} = \arg \min_{\mathbf{z} \in \mathbb{Z}^n} |\mathbf{F}_{dst} \mathbf{y}_{dst} + (\mathbf{B}_{dst} \mathbf{u} - \mathbf{B}_{dst} \mathbf{G} \mathbf{z})|^2 \quad (23)$$

where $n = 8M_u LT$. Then for the linear one-to-one relay mapper, we have

$$\mathbf{G} = \text{diag}(\mathbf{G}_1, \mathbf{G}_2, \mathbf{G}_3) \cdot \begin{pmatrix} \mathbf{I}_{2M_u LT} & \mathbf{0} & \mathbf{0} \\ \mathbf{0} & \mathbf{I}_{2M_u LT} & \mathbf{0} \\ \mathbf{I}_{4M_u LT} & \mathbf{0} & 2^{\frac{R}{2M_u}} \mathbf{I}_{4M_u LT} \end{pmatrix}. \quad (24)$$

For the linear modulo-sum relay mapper, with $M_u = M_r$, we choose the linear relay mapping such that $\tilde{\mathbf{z}}_3 = \tilde{\mathbf{z}}_1 + \tilde{\mathbf{z}}_2$ and the corresponding \mathbf{G} can be similarly derived. Note now that the decoder searches the whole integer vector plane \mathbb{Z}^n in (23), thus the lattice decoder using the efficient sphere decoding algorithm [11], [12] can be applied.

In the following simulation results, the number of slots is selected as $L = 2$, and the sum rate $(R_1 + R_2)$, is 4 BPCU. The relay forwards the message only when the users' messages are correctly decoded. All the channel links are Rayleigh faded and unless otherwise specified, the sources-to-relay (S-R) channel link is 10 dB better than the other channel links. In Fig. 3, for single-antenna nodes, we show that O-MLC has better error performance than that of MS-MLC and both outperform the protocols of [5], [9], [13] and [14] in terms of outage probability and achieve the diversity $\min\{M_u(M_r + N), (M_u + M_r)N\}$ as expected. In Fig. 4, for the cases $M_u = N = 1, M_r = 2$ and $M_u = M_r = 1, N = 2$ (where the S-R link is 15 dB better than the other channel links), respectively, we show that our proposed coding schemes outperform the MAF. For the former case, the MAF achieves a diversity of only 2 instead of 3. Note the methods in [9], [13] and [14] cannot be straightforwardly extended to the case of multiple-antenna nodes.

For the simulation of practical lattice codings based on one-stage practical decoder and linear relay mapper, with the slot length $T = 2$, we use the pair of self-similar randomly generated nested lattices drawn from the lattice ensemble defined in Definition 5. For the settings the same as the above, in Fig. 5, the block error rate for O-MLC and MS-MLC are presented. The parameters of the linear codes in the

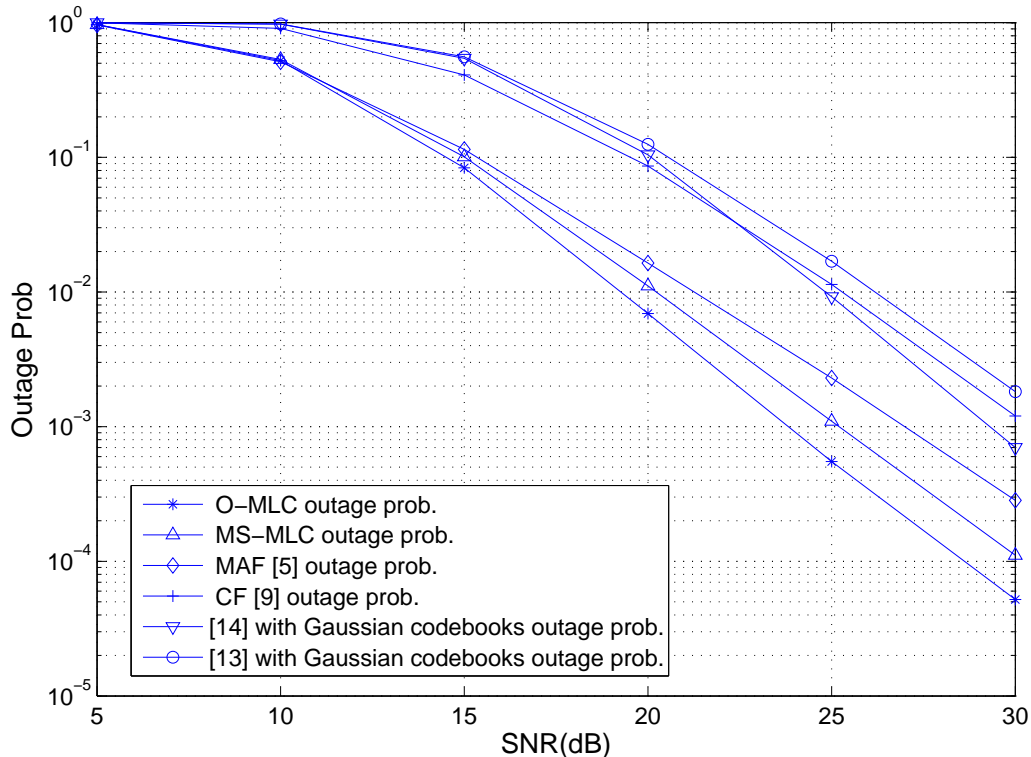


Fig. 3. The outage probability for O-MLC (14), (15) and MS-MLC (14), (15), (20) vs. the protocols in [5], [9], [13] and [14].

lattice ensemble for O-MLC and MS-MLC are $(p_i, k_i) = (97, 3), (47, 3), \forall i$ (cf. Definition 5), respectively. The diversity of 3 for each user is achieved as expected using our finite T code construction.

VI. CONCLUSION

In this work, we have proposed O-MLC and MS-MLC for structured MARC coding. The former enjoys better error performance, while the latter provides more flexibility to tradeoff between the complexity and the error performance. The error performance of MS-MLC can approach that of O-MLC by increasing the complexity. We have shown that with the new K -stage decoding instead of the one-stage decoding considered in previous works, the structured O-MLC can approach the rate performance of unstructured codebook with ML decoding. When only the one-stage decoder is used, O-MLC can still achieve the optimal DMT of DDF. Besides the theoretical results, we have also considered the design of practical short length lattice code with *linear* mapping, which facilitates the efficient lattice decoding. Simulation results have shown that our proposed coding schemes outperform existing schemes in terms of outage probabilities.

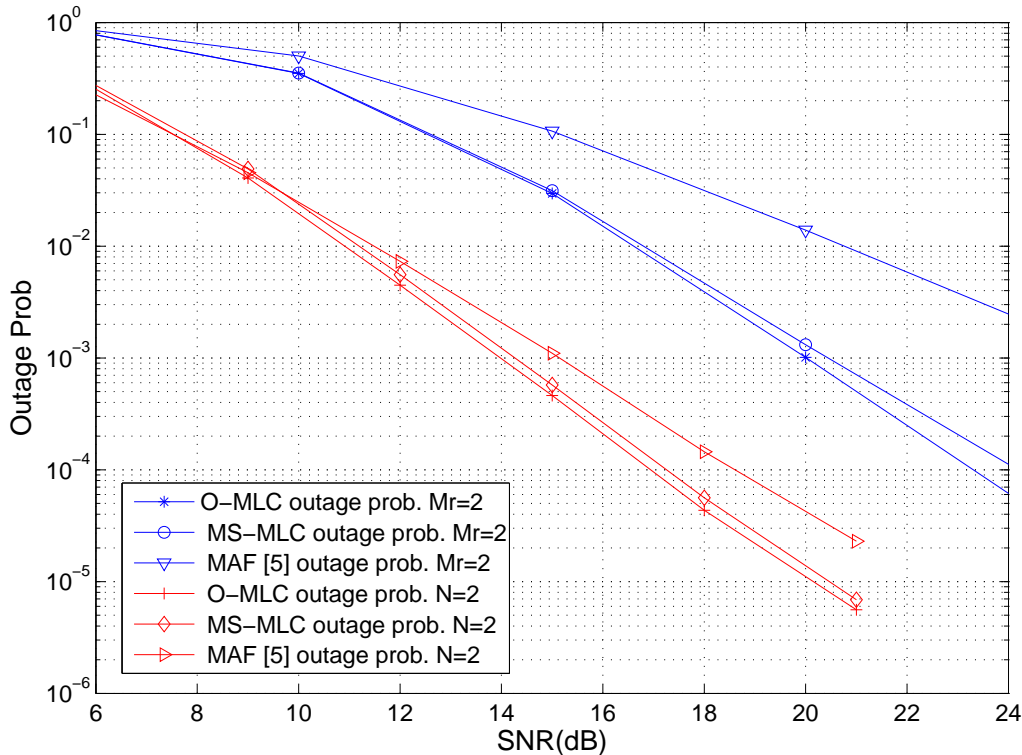


Fig. 4. The outage probability for O-MLC (14), (15) and MS-MLC (14), (15), (20) vs. MAF [5].

APPENDIX

A. Proof of Lemma 1

(I) Some useful definitions : Here we introduce some notation for simplification. We denote the nesting ratio in Definition 1 as $\tau_i = 2^{R_i/2M_u}$ while the dimensions of the lattice code are $n_i = 2M_uLT$, ($1 \leq i \leq K$). The corresponding parameters for the relay are τ_{K+1} and n_{K+1} , respectively. We also have the following definitions.

Definition 5 (Loeliger lattices ensemble [17]): Let $\bar{\Lambda}_{C_i}$ be a lattice generated by a linear code C_i^{Lo} as $\bar{\Lambda}_{C_i} \triangleq \{\mathbf{z} \in \mathbb{Z}^{n_i} : \bar{\mathbf{z}}_{p_i} \in C_i^{Lo}\}$, where $\bar{\mathbf{z}}_{p_i}$ is obtained by applying the componentwise reduction modulo p_i operation on \mathbf{z} [17] and the (n_i, k_i) linear code C_i^{Lo} is defined over the finite field $\mathbb{Z}_{p_i}^{n_i}$ ((T1.1) in Table I). The Loeliger lattices ensemble is the lattices ensemble $\{\Lambda_{C_i} = (\gamma_i \bar{\Lambda}_{C_i^{Lo}}) : C_i^{Lo} \in C_{i,Loe}, \gamma_i \in \mathbb{R}\}$, where $C_{i,Loe}$ is a balanced set of linear codes C_i^{Lo} [17]. In our analysis, we let $p_i \rightarrow \infty$, and $\gamma_i \rightarrow 0$ such that the fundamental volume of Λ_{C_i} ((T1.3) in Table I) $V_f(\Lambda_{C_i}) = p_i^{n_i - k_i} \gamma_i^{n_i}$ is fixed.

The following balanced set definition generalizes the balanced set defined in [17].

Definition 6: (Balanced set for the K-user MARC): Let C be the set of \mathbf{c} where $\mathbf{c} = \mathbf{c}_1 \times \cdots \times \mathbf{c}_{K+1} \in$

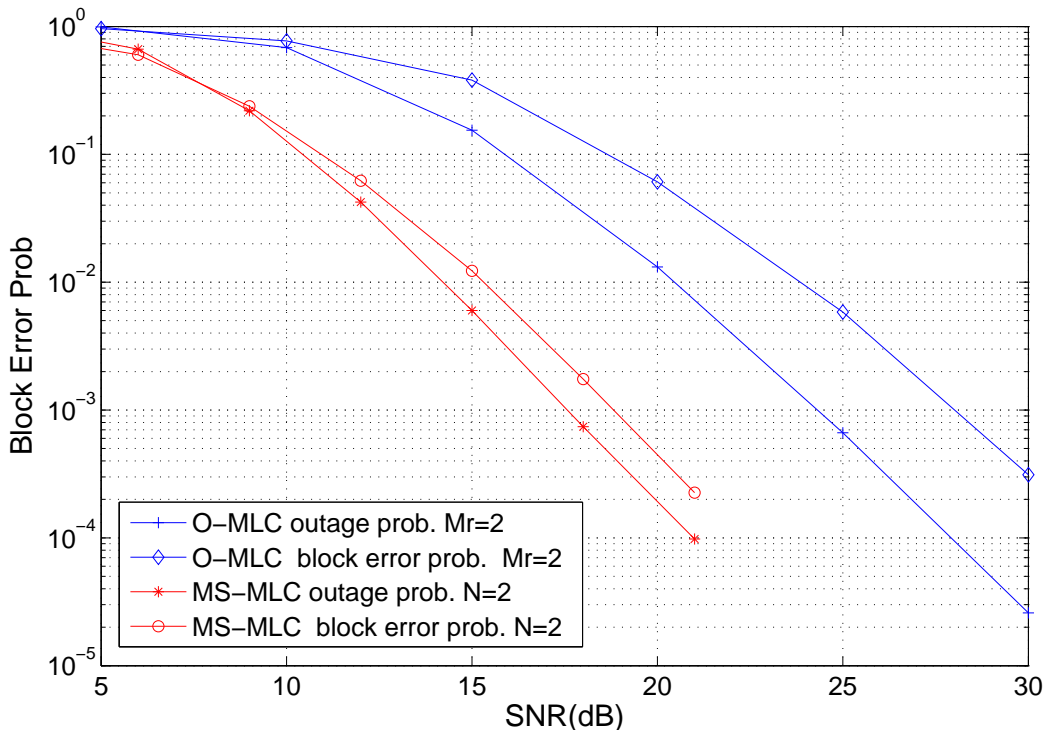


Fig. 5. Comparison of theoretical outage probabilities and the block error probabilities using practical linear relay mapping, (18), (19) for O-MLC and (18), (19), (21) for MS-MLC .

$\mathbb{R}^{n_1} \times \dots \times \mathbb{R}^{n_{K+1}}$, and \mathcal{C}_E be the finite set of C (e.g., \mathbf{c} is a codeword of a codebook C , and \mathcal{C}_E is a codebook ensemble). We collect all non-zero \mathbf{c} in C of \mathcal{C}_E as $(\mathcal{C}_E)^* \triangleq \{\mathbf{c} \in \mathbb{R}^n : \mathbf{c} \in C^*, C \in \mathcal{C}_E\}$, where $n = \sum_{i=1}^{K+1} n_i$, $C^* = C \setminus \{\mathbf{0}\}$. The set \mathcal{C}_E is called *balanced* if every nonzero element \mathbf{c} in $(\mathcal{C}_E)^*$ is contained in the same number, denoted by N_b , of C from \mathcal{C}_E . We refer to N_b as the *balanced number*.

(II) Proof: Here we show the proof only for the second inequality of (16) since the proof for the first one is similar to that in [10]. An outline of the proof is provided first to provide insight into how to solve the problem that cosets with set- $\mathcal{S}^{(1)}$ errors $\mathcal{O}_{\mathcal{S}^{(1)}}^{\Psi_{\Delta}^{one}} \triangleq \{\mathbf{d} \in \mathcal{O}_{\Psi_{\Delta}^{one}} : \bar{\mathbf{d}}_i \neq \mathbf{0}, \forall i \in \mathcal{S}^{(1)}\}$ (or even cosets $\mathcal{O}_{\Psi_{\Delta}^{one}}$ in (13)) is not a direct product of $K+1$ lattices, where the differential coset leader $\bar{\mathbf{d}}_i$ for user i is defined below (13) with (T1.4) and (T1.10) in Table I. First, by averaging over the ensemble of mappers, and judiciously using the balanced set property in Definition 6, we can upper bound $\frac{1}{|\mathcal{E}_{\Psi, CLo}|} \sum_{(\Psi_{\Delta}^{one}, C_{ur}^{Lo}) \in \mathcal{E}_{\Psi, CLo}} \left| \mathcal{O}_{\mathcal{S}^{(1)}}^{\Psi_{\Delta}^{one}} \cap \mathcal{R}_{\beta} \right|$ in (16) using the RHS of (27 b) below. Note that instead of summation over cosets $\mathcal{O}_{\mathcal{S}^{(1)}}^{\Psi_{\Delta}^{one}}$ as in the RHS of (26) below, in the RHS of (27 b) the summation is over the lattice points of set $(\Lambda_{C_{ur}})^*$ in (29) below, which makes further upper-bounding possible. By taking the limits, we conclude our proof.

Now we give the details to show the second inequality of (16). First we introduce some useful notation for the upcoming (25 a). The differential mapper Ψ_{Δ}^{one} , which corresponds to Ψ^{one} in Definition 2, is defined by replacing the super-codeword $\bar{\mathbf{c}} = [(\bar{\mathbf{c}}_u)^T, (\bar{\mathbf{c}}_r)^T]^T$ in Ψ^{one} with the differential super-codeword $\bar{\mathbf{d}}(\mathbf{w})$ in (13), as in (T1.14) of Table I. Let $\mathcal{E}_{\Psi_{\Delta}, C^{Lo}}$ be the ensemble corresponding to $\mathcal{E}_{\Psi, C^{Lo}}$ in (16), but with one-to-one mappers Ψ_{Δ}^{one} replaced by the corresponding differential mappers Ψ_{Δ}^{one} . Also let $f(\cdot)$ be the indicator function where $f(\mathbf{d}) = 1$ if $\mathbf{d} \in \mathcal{R}_{\beta}$, otherwise $f(\mathbf{d}) = 0$. Clearly the following (25 a) is valid for the left-hand side (LHS) of the second inequality of (16) since $|\mathcal{E}_{\Psi, C^{Lo}}| = |\mathcal{E}_{\Psi_{\Delta}, C^{Lo}}|$,

$$\frac{1}{|\mathcal{E}_{\Psi, C^{Lo}}|} \sum_{(\Psi_{\Delta}^{one}, C_{ur}^{Lo}) \in \mathcal{E}_{\Psi, C^{Lo}}} \left| \mathbb{O}_{\mathcal{S}^{(1)}}^{\Psi_{\Delta}^{one}} \cap \mathcal{R}_{\beta} \right| \stackrel{(a)}{=} \sum_{(\Psi_{\Delta}^{one}, C_{ur}^{Lo}) \in \mathcal{E}_{\Psi_{\Delta}, C^{Lo}}} \sum_{\mathbf{d} \in \mathbb{O}_{\Delta, \mathcal{S}^{(1)}}^{\Psi_{\Delta}^{one}}} \frac{f(\mathbf{d})}{|\mathcal{E}_{\Psi_{\Delta}, C^{Lo}}|} \stackrel{(b)}{\leq} \frac{(\tau_{K+1})^{n_{K+1}} \prod_{i \in \mathcal{S}^{(1)}} 2^{R_i L T}}{(\tau_{K+1})^{n_{K+1}} - 1} \frac{\int_{\mathbb{R}^{\sum_{i=1}^{K+1} n_i}} f(\mathbf{d}) d\mathbf{d}}{\prod_{i \in \{\mathcal{S}^{(1)}, K+1\}} V_{f(\Lambda_{S_i})}}. \quad (25)$$

As for the above (25 b), it can be proved from the RHS of the upcoming (27 b) by averaging over C_{Loe} using techniques similar to those in [10] and [17]. Thus we focus on the proof of (27 b) below. As pointed out in the beginning of this appendix, our trick to prove this *critical* step is replacing the summation over the “non-lattice” cosets $\mathbb{O}_{\mathcal{S}^{(1)}}^{\Psi_{\Delta}^{one}}$ in the LHS of (25 b) with the set $(\Lambda_{C_{ur}})^*$ in (27 b) by showing

$$\frac{1}{|\mathcal{E}_{\Psi_{\Delta}, C^{Lo}}|} \sum_{(\Psi_{\Delta}^{one}, C_{ur}^{Lo}) \in \mathcal{E}_{\Psi_{\Delta}, C^{Lo}}} \sum_{\mathbf{d} \in \mathbb{O}_{\mathcal{S}^{(1)}}^{\Psi_{\Delta}^{one}}} f(\mathbf{d}) = \frac{1}{|C_{Loe}|} \sum_{C_{ur}^{Lo} \in C_{Loe}} \left(\frac{1}{|C_{\Psi_{\Delta}, E}|} \sum_{\Psi_{\Delta}^{one} \in \Psi_{\Delta}^{one}} \sum_{\mathbf{d} \in \mathbb{O}_{\mathcal{S}^{(1)}}^{\Psi_{\Delta}^{one}}} f(\mathbf{d}) \right) \quad (26)$$

$$\stackrel{(a)}{=} \frac{1}{|C_{Loe}|} \sum_{C_{ur}^{Lo} \in C_{Loe}} \left(\frac{1}{((\tau_{K+1})^{n_{K+1}} - 1)} \sum_{\mathbf{d} \in (\Lambda_{C_{ur}})^{\diamond}} f(\mathbf{d}) \right) \stackrel{(b)}{\leq} \frac{1}{((\tau_{K+1})^{n_{K+1}} - 1) |C_{Loe}|} \sum_{C_{ur}^{Lo} \in C_{Loe}} \sum_{\mathbf{d} \in (\Lambda_{C_{ur}})^*} f(\mathbf{d}), \quad (27)$$

where the derivation of each step comes as follows:

For (26), we first define $C_{\Psi_{\Delta}, E}$ as the ensemble of all mapped nested-codebooks (differential) $C_{\Psi_{\Delta}^{one}}$ given a particular super Loeliger linear code C_{ur}^{Lo} (T1.6), with codewords of $C_{\Psi_{\Delta}^{one}}$ satisfying the mapping rules of the corresponding Ψ_{Δ}^{one} . Note that all $C_{\Psi_{\Delta}^{one}} \in C_{\Psi_{\Delta}, E}$ are based on the same C_{ur}^{Lo} , but with different mappers. Also let $C_{Loe} = C_{1,Loe} \times \cdots \times C_{K+1,Loe}$ be the ensemble of all possible C_{ur}^{Lo} with $C_{i,Loe}$ given in Definition 5, and Ψ_{Δ}^{one} be the ensemble of all possible differential mappers. Then (26) is obtained by $|\mathcal{E}_{\Psi_{\Delta}, C^{Lo}}| = |C_{\Psi_{\Delta}, E}| |C_{Loe}|$ by definition.

For (27 a), given mapper Ψ_{Δ}^{one} and Loeliger linear code C_{ur}^{Lo} (thus mapped-codebook $C_{\Psi_{\Delta}^{one}}$), we rewrite the set- $\mathcal{S}^{(1)}$ error cosets as $\mathbb{O}_{\mathcal{S}^{(1)}}^{\Psi_{\Delta}^{one}} = \{\mathbf{d} \in \Lambda_{C_{ur}} : \bar{\mathbf{d}} \in C_{\Psi_{\Delta}^{one}}^*, \bar{\mathbf{d}}_i \neq \mathbf{0}, \forall i \in \mathcal{S}^{(1)}\}$, where $\Lambda_{C_{ur}}$ is in (T1.9), and set- $\mathcal{S}^{(1)}$ errors is defined in Definition 4. Then the term inside the parentheses on the LHS of (27 a) comes

from

$$\frac{1}{|C_{\Psi_{\Delta,E}}|} \sum_{\Psi_{\Delta}^{one} \in \Psi_{\Delta}^{one}} \sum_{\mathbf{d} \in \mathcal{O}_{\mathcal{S}^{(1)}}^{\Psi_{\Delta}^{one}}} f(\mathbf{d}) = \frac{1}{|C_{\Psi_{\Delta,E}}|} \left(N_b \sum_{\mathbf{d} \in (\Lambda_{C_{ur}})^{\diamond}} f(\mathbf{d}) \right) \quad (28)$$

where we collect all points belonging to cosets $\mathcal{O}_{\mathcal{S}^{(1)}}^{\Psi_{\Delta}^{one}}$ over all possible mapped codebooks $C_{\Psi_{\Delta}^{one}}$ as $(\Lambda_{C_{ur}})^{\diamond} \triangleq \left\{ \mathbf{d} \in \Lambda_{C_{ur}} : \mathbf{d} \in \mathcal{O}_{\mathcal{S}^{(1)}}^{\Psi_{\Delta}^{one}}, C_{\Psi_{\Delta}^{one}} \in C_{\Psi_{\Delta,E}} \right\}$. For (28), it comes from the fact that $C_{\Psi_{\Delta,E}}$ is a balanced set as follows, where $(C_{C_{\Psi_{\Delta,E}}})^*$ is the collection of non-zero codewords in $C_{\Psi_{\Delta,E}}$, by setting $(C_{C_E})^*$ in Definition 6 with $C_E = C_{\Psi_{\Delta,E}}$ ((T1.15) in Table I). Consider two different vectors \mathbf{c} and \mathbf{c}' belonging to $(C_{C_{\Psi_{\Delta,E}}})^*$. For each mapped-codebook $C_{\Psi_{\Delta}^{one}} \in C_{\Psi_{\Delta,E}}$ containing \mathbf{c} but not \mathbf{c}' , with the corresponding mapper Ψ_{Δ}^{one} , we can easily form another $C_{(\Psi_{\Delta}^{one})'} \in C_{\Psi_{\Delta,E}}$ containing \mathbf{c}' by forming a new one-to-one mapper $(\Psi_{\Delta}^{one})'$ from Ψ_{Δ}^{one} . Therefore, \mathbf{c} and \mathbf{c}' are symmetric, and thus each vector in $(C_{C_{\Psi_{\Delta,E}}})^*$ is contained in equal number, denoted by N_b , of $C_{\Psi_{\Delta}^{one}}$ from $C_{\Psi_{\Delta,E}}$. Then $C_{\Psi_{\Delta,E}}$ is a balanced set as in Definition 6. Together with the fact that $(C_{C_{\Psi_{\Delta,E}}})^*$ is the set of coset leaders of $(\Lambda_{C_{ur}})^{\diamond}$, that is, $(C_{C_{\Psi_{\Delta,E}}})^* = \{\bar{\mathbf{d}} : \mathbf{d} \in (\Lambda_{C_{ur}})^{\diamond}\}$, then (28) follows. Finally, with $(\tau_{K+1})^{n_{K+1}}$ being the relay codebook size, since the differential mapper Ψ_{Δ}^{one} is one-to-one, each nonzero user codeword can possibly be mapped to $(\tau_{K+1})^{n_{K+1}} - 1$ relay codewords. Also the mapped nested-codebook ensemble $C_{\Psi_{\Delta,E}}$ is a balanced set with balanced number N_b , we have that $|C_{\Psi_{\Delta,E}}|/N_b = (\tau_{K+1})^{n_{K+1}} - 1$. Then we obtain (27 a) from (28).

For (27 b), we define $(\Lambda_{C_{ur}})^*$ formed from the super coding-lattice $\Lambda_{C_{ur}}$ ((T1.9) in Table I) as

$$(\Lambda_{C_{ur}})^* \triangleq \left\{ \mathbf{d} \in \Lambda_{C_{ur}} : \mathbf{d}_i \neq \mathbf{0}, \forall i \in \mathcal{S}^{(1)} \right\}. \quad (29)$$

From the definition of $(\Lambda_{C_{ur}})^{\diamond}$ right after (28), we have $(\Lambda_{C_{ur}})^{\diamond} \subset (\Lambda_{C_{ur}})^*$. Together with the fact that the indicator function $f(\cdot)$, defined right before (25), is a nonnegative function, (27 b) is obtained.

Finally, the second inequality of (16) can be obtained from (25 b) by following steps similar to those in [10] and [16]. The key observation is that as $T \rightarrow \infty$, the shaping lattices Λ_{S_i} from Definitions 1 and 5 will be good for minimum square error quantization [22], so that their Voronoi regions $V_f(\Lambda_{S_i})$ will make the signal behave like an optimal Gaussian signal. Thus the term $\frac{1}{LT} \log \int_{\mathbb{R}^{\sum_{i=1}^{K+1} n_i}} f(\mathbf{d}) d\mathbf{d} / \prod_{i \in \{\mathcal{S}^{(1)}, K+1\}} V_f(\Lambda_{S_i})$ in (25 b) will approach $-\frac{1}{LT} R_{unG}^{dst}(\mathbf{H}_{dst}^{\{\mathcal{S}^{(1)}, K+1\}})$ in (16). With $(\tau_{K+1})^{n_{K+1}} = 2^{R_{K+1}LT}$ as defined in Appendix A-(I), we then have the second inequality of (16). The details are given in Appendix C.

B. Proof of the rate region of the K-stage MS-MLC in Theorem 2

The proof for the rate region of MS-MLC is similar to the proof of Theorem 1. Here we show only the principal difference, which results from the fact that the balanced set structure exploited in Appendix A (to obtain (28)) is no longer valid for MS-MLC. We solve this problem by introducing a new 2-partition balanced set defined in Definition 7 below. Specifically, we will show a counterpart of (25) for the first stage as follows: For MS-MLC, with the relay-mapper and linear-code ensemble $\mathcal{E}_{\Psi, C^{Lo}}$ of $\{\Psi^{mod}, C_{ur}^{Lo}\}$ and $\mathcal{S}^{(1)} = \{1, \dots, K\}$, we have

$$\begin{aligned} & \frac{1}{|\mathcal{E}_{\Psi, C^{Lo}}|} \sum_{(\Psi^{mod}, C_{ur}^{Lo}) \in \mathcal{E}_{\Psi, C^{Lo}}} \left| \mathcal{O}_{\mathcal{S}^{(1)}}^{\Psi^{mod}} \cap \mathcal{R}_{\beta} \right| \\ & \leq \frac{(\tau_{K+1})^{n_{K+1}} \prod_{i \in \mathcal{S}^{(1)}} 2^{R_i LT}}{((\tau_{K+1})^{n_{K+1}} - 1)} \left(\frac{\int_{\mathbb{R}^{\sum_{i=1}^{K+1} n_i}} f(\mathbf{d}) d\mathbf{d}}{\prod_{i \in \{\mathcal{S}^{(1)}, K+1\}} V_f(\Lambda_{S_i})} + \frac{\int_{\mathbb{R}^{\sum_{i=1}^K n_i}} f^{\mathcal{S}^{(1)}}(\mathbf{d}_{\mathcal{S}^{(1)}}) d\mathbf{d}_{\mathcal{S}^{(1)}}}{(\tau_{K+1})^{n_{K+1}} \prod_{i \in \mathcal{S}^{(1)}} V_f(\Lambda_{S_i})} \right), \end{aligned} \quad (30)$$

which, compared with (25), has an additional term (second term) in the RHS, (30) where we let $\mathbf{d}_{\mathcal{S}^{(1)}} = [\mathbf{d}_{i_1}^T, \dots, \mathbf{d}_{i_{|\mathcal{S}^{(1)}|}}^T]^T$, $i_1 < \dots < i_{|\mathcal{S}^{(1)}|}$, $\forall i_j \in \mathcal{S}^{(1)}$, and the indicator function $f^{\mathcal{S}^{(1)}}(\mathbf{d}_{\mathcal{S}^{(1)}}) = 1$ if $\mathbf{d}_{\mathcal{S}^{(1)}} \in \mathcal{R}_{\beta}^{\mathcal{S}^{(1)}}$, with $\mathcal{R}_{\beta}^{\mathcal{S}^{(1)}} \triangleq \left\{ \mathbf{v}_{\mathcal{S}^{(1)}} \in \mathbb{R}^{2|\mathcal{S}^{(1)}| M_u LT} : \mathbf{v} \in \mathcal{R}_{\beta}, \mathbf{v}_i = \mathbf{0}, \forall i \in \{\{1, \dots, K+1\} \setminus \mathcal{S}^{(1)}\} \right\}$ and the decision region \mathcal{R}_{β} given in Lemma 1. This additional term results in the additional rate constraint (20) compared with Theorem 1. Similar to the derivations of (25 a) and (26), the LHS of (30) equals

$$\frac{1}{|\mathcal{E}_{\Psi, C^{Lo}}|} \sum_{(\Psi^{mod}, C_{ur}^{Lo}) \in \mathcal{E}_{\Psi, C^{Lo}}} \left| \mathcal{O}_{\mathcal{S}^{(1)}}^{\Psi^{mod}} \cap \mathcal{R}_{\beta} \right| = \frac{1}{|C_{Loe}|} \sum_{C_{ur}^{Lo} \in C_{Loe}} \left(\frac{1}{|C_{\Psi_{\Delta}, E}|} \sum_{\Psi_{\Delta}^{mod} \in \Psi_{\Delta}^{mod}} \sum_{\mathbf{d} \in \mathcal{O}_{\mathcal{S}^{(1)}}^{\Psi_{\Delta}^{mod}}} f(\mathbf{d}) \right). \quad (31)$$

Compared with (26), only the (differential) one-to-one mapper Ψ_{Δ}^{one} is replaced by Ψ_{Δ}^{mod} in (31). However, unlike O-MLC in Appendix A, now $C_{\Psi_{\Delta}, E}$ is not a balanced set, which makes simplifying (31) more difficult compared with (27 a). To solve this problem, we need to extend Definition 6 as follows.

Definition 7: (2-partition balanced set): Following the notation in Definition 6, we say that the set C_E is 2-partition balanced if the non-zero vector set $(C_{C_E})^*$ can be partitioned as $(C_{C_E})^* = \{C_{C_E,1}^*, C_{C_E,2}^*\}$, where every element in $C_{C_E,1}^*$ is contained in the same number, denoted by $N_{b,1}$, of C from C_E while every element in $C_{C_E,2}^*$ is also contained in the same number, denoted by $N_{b,2}$, of C from C_E .

For simplifying the RHS of (31), now we explore the properties of the ensemble $C_{\Psi_{\Delta}, E}$ using the 2-partition balanced set in Definition 7. Recall that $C_{\Psi_{\Delta}, E}$ is the ensemble of all mapper-codebooks (differential) $C_{\Psi_{\Delta}^{mod}}$ with mapper $\Psi_{\Delta}^{mod} \in \Psi_{\Delta}^{mod}$, where the differential super-codewords in $C_{\Psi_{\Delta}^{mod}}$ satisfy the

mapping rules of Ψ_{Δ}^{mod} . For any user set $S \subseteq \{1, \dots, K\}$, let $\mathcal{C}_{\Psi_{\Delta}, E}^S$ be the set of mapper-codebooks formed by collecting every codebook belonging to $\mathcal{C}_{\Psi_{\Delta}, E}$, but excluding codewords $\bar{\mathbf{d}} \notin \mathcal{D}_S$ where $\mathcal{D}_S \triangleq \{\bar{\mathbf{d}} : \bar{\mathbf{d}}_i \neq \mathbf{0}, \forall i \in S\}$. The fact that for every user set S , $\mathcal{C}_{\Psi_{\Delta}, E}^S$ is a 2-partition balanced set in Definition 7 follows from the following observations. According to whether the differential codewords of the relay $\bar{\mathbf{d}}_r = \mathbf{0}$ or not, we can categorize them into two partitions. The differential codewords in each partition are symmetric according to the proof in Appendix A. Note that $\bar{\mathbf{d}}_r = \mathbf{0}$ occurs only in the MS-MLC due to the modulo-sum operation in Definition 3. In O-MLC, the one-to-one mapper guarantees $\bar{\mathbf{d}}_r \neq \mathbf{0}$, and results in simpler (25) compared with our target (30). Now for the first stage, we set $S = \mathcal{S}^{(1)}$ and the two partitions of $\mathcal{C}_{\Psi_{\Delta}, E}^{\mathcal{S}^{(1)}}$ can be formed as follows. Let $\mathcal{C}_{\Psi_{\Delta}, E, 1}^{\mathcal{S}^{(1)}}$ and $\mathcal{C}_{\Psi_{\Delta}, E, 2}^{\mathcal{S}^{(1)}}$ be the codeword partitions corresponding to $\mathcal{C}_{\mathcal{C}_E, 1}^*$ and $\mathcal{C}_{\mathcal{C}_E, 2}^*$ in Definition 7 with $\mathcal{C}_E = \mathcal{C}_{\Psi_{\Delta}, E}^{\mathcal{S}^{(1)}}$ respectively, where $\mathcal{C}_{\Psi_{\Delta}, E, 1}^{\mathcal{S}^{(1)}} = \{\bar{\mathbf{d}} \in \mathcal{C}_{\Psi_{\Delta}}^{*mod} : \bar{\mathbf{d}}_r \neq \mathbf{0}, \bar{\mathbf{d}} \in \mathcal{D}_{\mathcal{S}^{(1)}}, \Psi_{\Delta}^{mod} \in \Psi_{\Delta}^{mod}\}$, where the codewords of the relay are distinguishable since $\bar{\mathbf{d}}_r \neq \mathbf{0}$; $\mathcal{C}_{\Psi_{\Delta}, E, 2}^{\mathcal{S}^{(1)}}$ is defined similarly but with $\bar{\mathbf{d}}_r \neq \mathbf{0}$ replaced by $\bar{\mathbf{d}}_r = \mathbf{0}$. Also let the corresponding balanced numbers of $\mathcal{C}_{\mathcal{C}_E, 1}^*$ and $\mathcal{C}_{\mathcal{C}_E, 2}^*$ be $N_{b,1}$ and $N_{b,2}$ respectively. Now we can simplify the RHS of (31) using the aforementioned 2-partition balanced set property and following the proof of the O-MLC counterpart (28), while in (28) $\mathcal{C}_{\Psi_{\Delta}, E}$ is a balanced set. Corresponding to (28), the term inside the parentheses on the RHS of (31) now equals

$$\sum_{\Psi_{\Delta}^{mod} \in \Psi_{\Delta}^{mod}} \sum_{\mathbf{d} \in \mathcal{O}_{\Delta, \mathcal{S}^{(1)}}^{mod}} \frac{f(\mathbf{d})}{|\mathcal{C}_{\Psi_{\Delta}, E}|} = \frac{N_{b,1}}{|\mathcal{C}_{\Psi_{\Delta}, E}|} \sum_{\mathbf{d} \in (\Lambda_{\mathcal{C}_{ur}, 1})^{\diamond}} f(\mathbf{d}) + \frac{N_{b,2}}{|\mathcal{C}_{\Psi_{\Delta}, E}|} \sum_{\mathbf{d} \in (\Lambda_{\mathcal{C}_{ur}, 2})^{\diamond}} f(\mathbf{d}) \quad (32)$$

where $(\Lambda_{\mathcal{C}_{ur}, 1})^{\diamond}$ and $(\Lambda_{\mathcal{C}_{ur}, 2})^{\diamond}$ are the lattice codeword sets for the 2-partitions corresponding to $(\Lambda_{\mathcal{C}_{ur}})^{\diamond}$ in (28), respectively.

Unfortunately, the balanced numbers in (32) cannot be easily computed as in the proof of (27 a) and vary with $\mathcal{C}_{\Psi_{\Delta}, E}^S$ for different sets S . Thus we alternatively show two upper-bounds as

$$\frac{N_{b,1}}{|\mathcal{C}_{\Psi_{\Delta}, E}|} \leq \frac{1}{(\tau_{K+1})^{n_{K+1}} - 1}, \text{ and } \frac{N_{b,2}}{|\mathcal{C}_{\Psi_{\Delta}, E}|} \leq \frac{1}{(\tau_{K+1})^{n_{K+1}} - 1}, \quad (33)$$

where $(\tau_{K+1})^{n_{K+1}}$ is the relay codebook size from Definition 1. Then following similar arguments as those used in proving (27 a), (27 b) and (25 b) (steps after (28)), we can prove (30) from (32) and (33) with the details omitted. For proving (33), we start with the single user case where $|\mathcal{S}^{(1)}| = 1$ ($\mathcal{S}^{(1)} = \{1, \dots, K\} = \{1\}$ when the number of users $K = 1$), and then extend to the case $|\mathcal{S}^{(1)}| = 2$ as the upcoming (34) and (35). By repeating this procedure recursively, we obtain the formulation of balanced

numbers in (33) as (36) in the next paragraph and then derive the upper-bound. When $|\mathcal{S}^{(1)}| = 1$, $\mathcal{C}_{\Psi_{\Delta},E}$ is a balanced set, and thus balanced numbers (normalized) are given by $(N_{b,1}/|\mathcal{C}_{\Psi_{\Delta},E}|)_{|\mathcal{S}^{(1)}|=1} = \frac{1}{((\tau_{K+1})^{n_{K+1}-1})}$ from the proof of (27 a), and $(N_{b,2}/|\mathcal{C}_{\Psi_{\Delta},E}|)_{|\mathcal{S}^{(1)}|=1} = 0$ by definition. Here the subscript $|\mathcal{S}^{(1)}| = 1$ is added to the notation of the normalized balanced numbers to represent the upcoming (34) and (35). For $|\mathcal{S}^{(1)}| = 2$, the corresponding balanced number for the partition with $\bar{\mathbf{d}}_r = \mathbf{0}$ is

$$\left(\frac{N_{b,2}}{|\mathcal{C}_{\Psi_{\Delta},E}|} \right)_{|\mathcal{S}^{(1)}|=2} = \frac{1}{((\tau_3)^{n_3} - 1)} \left(((\tau_3)^{n_3} - 1) \left(\frac{N_{b,1}}{|\mathcal{C}_{\Psi_{\Delta},E}|} \right)_{|\mathcal{S}^{(1)}|=1} \right). \quad (34)$$

To show (34), we count the occurrence of a particular super-codeword (differential) $\bar{\mathbf{d}}_1 \times \bar{\mathbf{d}}_2 \times \mathbf{0}$ ($\bar{\mathbf{d}}_r = \mathbf{0}$) in the overall two-user mapped-codebook ensemble $\mathcal{C}_{\Psi_{\Delta},E}$, where user i 's codeword (coset leader) is $\bar{\mathbf{d}}_i$, $i = 1, 2$. Let $\Psi_{\Delta,i}^{mod}(\bar{\mathbf{d}}_i)$ be the (differential) mapper corresponding to user i as in Definition 3. First, we compute $\frac{(N_{b,2})_{|\mathcal{S}^{(1)}|=2}}{(N_{b,1})_{|\mathcal{S}^{(1)}|=1}}$. From Definition 6, given a particular $\bar{\mathbf{d}}_1 \times \bar{\mathbf{d}}_{r,1}$ with $\bar{\mathbf{d}}_1 \neq \mathbf{0}$ such that $\bar{\mathbf{d}}_{r,1} = \Psi_{\Delta,1}^{mod}(\bar{\mathbf{d}}_1)$, there will be $(N_{b,1})_{|\mathcal{S}^{(1)}|=1}$ possible mappers $\Psi_{\Delta,1}^{mod}$. Now from Definition 3, for this partition to have $\bar{\mathbf{d}}_r = \sum_{i=1}^2 \Psi_{\Delta,i}^{mod}(\bar{\mathbf{d}}_i) = \mathbf{0}$, the mappers corresponding to user 2 must satisfy $(\bar{\mathbf{d}}_{r,1} + \Psi_{\Delta,2}^{mod}(\bar{\mathbf{d}}_2)) \bmod \Lambda_{S_r} = \mathbf{0}$ since $\bar{\mathbf{d}}_{r,1} = \Psi_{\Delta,1}^{mod}(\bar{\mathbf{d}}_1)$. Thus for a fixed $\bar{\mathbf{d}}_{r,1}$, the vector $\Psi_{\Delta,2}^{mod}(\bar{\mathbf{d}}_2)$ for the given $\bar{\mathbf{d}}_2$ is also fixed from the definition of the codomain C_r^{nest} of $\Psi_{\Delta,2}^{mod}(\cdot)$ given in Definition 2. Also from Definition 4, $\bar{\mathbf{d}}_2 \neq \mathbf{0}$ since the user messages (encoded in cosets) are with set- $\mathcal{S}^{(1)}$ errors, where $\mathcal{S}^{(1)} = \{1, 2\}$. Then for a fixed $\bar{\mathbf{d}}_{r,1}$, excluding the given $\bar{\mathbf{d}}_2$ and the zero vector, by assigning the mapping rules for the remaining $(\tau_2)^{n_2} - 2$ points in the domain of $\Psi_{\Delta,2}^{mod}(\cdot)$, there are $\prod_{i=2}^{(\tau_2)^{n_2}-1} ((\tau_3)^{n_3} - i)$ possible injective mappers $\Psi_{\Delta,2}^{mod}$ where $(\tau_i)^{n_i}$ is transmitter i 's (users and relay) codebook size. Note that to make $(\Psi_{\Delta,2}^{mod}(\bar{\mathbf{d}}_2) + \bar{\mathbf{d}}_{r,1}) \bmod \Lambda_{S_r} = \mathbf{0}$, it is required that $\bar{\mathbf{d}}_{r,1} \neq \mathbf{0}$ since $\bar{\mathbf{d}}_2 \neq \mathbf{0}$. As there are a total of $((\tau_3)^{n_3} - 1)$ possible $\bar{\mathbf{d}}_{r,1} \neq \mathbf{0}$ in the relay's (differential) codebook, we have $\frac{(N_{b,2})_{|\mathcal{S}^{(1)}|=2}}{(N_{b,1})_{|\mathcal{S}^{(1)}|=1}} = ((\tau_3)^{n_3} - 1) \prod_{i=2}^{(\tau_2)^{n_2}-1} ((\tau_3)^{n_3} - i)$. Also $\frac{|\mathcal{C}_{\Psi_{\Delta},E}|_{|\mathcal{S}^{(1)}|=2}}{|\mathcal{C}_{\Psi_{\Delta},E}|_{|\mathcal{S}^{(1)}|=1}} = ((\tau_3)^{n_3} - 1) \prod_{i=2}^{(\tau_2)^{n_2}-1} ((\tau_3)^{n_3} - i)$ by counting all possible injective mappers $\Psi_{\Delta,2}^{mod}$ of user 2. Thus (34) is valid. Similar to (34), for $|\mathcal{S}^{(1)}| = 2$, the corresponding balanced number for the partition with $\bar{\mathbf{d}}_r \neq \mathbf{0}$ is

$$\left(\frac{N_{b,1}}{|\mathcal{C}_{\Psi_{\Delta},E}|} \right)_{|\mathcal{S}^{(1)}|=2} = \frac{1}{((\tau_3)^{n_3} - 1)} \left(((\tau_3)^{n_3} - 2) \left(\frac{N_{b,1}}{|\mathcal{C}_{\Psi_{\Delta},E}|} \right)_{|\mathcal{S}^{(1)}|=1} + 1 \cdot \left(\frac{N_{b,2}}{|\mathcal{C}_{\Psi_{\Delta},E}|} \right)_{|\mathcal{S}^{(1)}|=1} \right). \quad (35)$$

The proof of (35) is similar to that for (34), but now $(\Psi_{\Delta,2}^{mod}(\bar{\mathbf{d}}_2) + \bar{\mathbf{d}}_{r,1}) \bmod \Lambda_{S_r} \neq \mathbf{0}$. The first term in the parenthesis on the RHS of (35) corresponds to the case $\bar{\mathbf{d}}_{r,1} \neq \mathbf{0}$ while the second term corresponds to the case $\bar{\mathbf{d}}_{r,1} = \mathbf{0}$. The details are omitted.

Finally, by repeating the arguments in the previous paragraph we can find the balanced numbers for $|\mathcal{S}^{(1)}| = 3$ with (34) and (35), and so on. Then for the balanced numbers when $|\mathcal{S}^{(1)}| = K$, we have

$$\begin{aligned} \frac{N_{b,1}}{|\mathcal{C}_{\Psi_{\Delta},\mathbf{E}}|} &= \frac{1}{(\tau_{K+1})^{n_{K+1}}((\tau_{K+1})^{n_{K+1}} - 1)^{|\mathcal{S}^{(1)}|}} \left(((\tau_{K+1})^{n_{K+1}} - 1)^{|\mathcal{S}^{(1)}|} + (-1)^{|\mathcal{S}^{(1)}|+1} \right) \\ \frac{N_{b,2}}{|\mathcal{C}_{\Psi_{\Delta},\mathbf{E}}|} &= \frac{1}{(\tau_{K+1})^{n_{K+1}}((\tau_{K+1})^{n_{K+1}} - 1)^{|\mathcal{S}^{(1)}|}} \left(((\tau_{K+1})^{n_{K+1}} - 1)^{|\mathcal{S}^{(1)}|} + ((\tau_{K+1})^{n_{K+1}} - 1)(-1)^{|\mathcal{S}^{(1)}|} \right), \end{aligned} \quad (36)$$

where $(\tau_{K+1})^{n_{K+1}}$ is the relay codebook size. On noting that $\frac{1}{((\tau_{K+1})^{n_{K+1}} - 1)^{|\mathcal{S}^{(1)}|}} \leq \frac{1}{(\tau_{K+1})^{n_{K+1}} - 1}$ for $|\mathcal{S}^{(1)}| \geq 1$, together with (36), one can show that (33) is valid. Then our proof for (30) is complete.

C. Proof of (25 b) and (16)

We can rewrite (27) as

$$\begin{aligned} & \frac{1}{((\tau_{K+1})^{n_{K+1}} - 1)^{|\mathcal{C}_{Loe}|}} \sum_{C_{ur}^{Lo} \in \mathcal{C}_{Loe}} \sum_{\mathbf{d} \in (\Lambda_{C_{ur}})^*} f(\mathbf{d}) \\ &= \frac{1}{((\tau_{K+1})^{n_{K+1}} - 1)} \sum_{\mathbf{z} \in (\mathbb{Z}^n)^* : \bar{\mathbf{z}}_{\underline{p}} = \mathbf{0}} f(\underline{\gamma}\mathbf{z}) + \frac{1}{|\mathcal{C}_{Loe}|} \sum_{C_{ur}^{Lo} \in \mathcal{C}_{Loe}} \sum_{\mathbf{a} \in (C_{ur}^{Lo})^*} \left[\sum_{\mathbf{z} \in (\mathbb{Z}^n)^* : \bar{\mathbf{z}}_{\underline{p}} = \mathbf{a}} f(\underline{\gamma}\mathbf{z}) \right], \end{aligned} \quad (37)$$

where $\underline{\gamma}\mathbf{z}$ is defined in (T1.23) in Table I. In (38), we define $(\mathbb{Z}^n)^* \triangleq \{\mathbf{z} \in \mathbb{Z}^n : \mathbf{z}_i \neq \mathbf{0}, \forall i \in \{1, \dots, K+1\}\}$ and $\bar{\mathbf{z}}_{\underline{p}}$ is formed by applying modulo p_i operation on elements of \mathbf{z}_i ((T1.22) in Table I). Now for summation in the second term of (38), we separate the summation over $\mathbf{a} \in (C_{ur}^{Lo})^*$ by the cases $\{\mathbf{a}_u \neq \mathbf{0}, \mathbf{a}_r = \mathbf{0}\}$, $\{\mathbf{a}_r \neq \mathbf{0}, \mathbf{a}_u = \mathbf{0}\}$ and $\{\mathbf{a}_r \neq \mathbf{0}, \mathbf{a}_u \neq \mathbf{0}\}$. By averaging over \mathcal{C}_{Loe} for these three cases, we have (39), (40) and (41), respectively,

$$\begin{aligned} & \frac{1}{|\mathcal{C}_{Loe}|} \sum_{C_{ur}^{Lo} \in \mathcal{C}_{Loe}} \sum_{\mathbf{a} \in (C_{ur}^{Lo})^*} \left[\sum_{\mathbf{z} \in (\mathbb{Z}^n)^* : \bar{\mathbf{z}}_{\underline{p}} = \mathbf{a}} f(\underline{\gamma}\mathbf{z}) \right] \\ &= \sum_{S \subseteq \{1, \dots, K\}, S \neq \emptyset} \left[\frac{\prod_{i \in S} (p_i^{k_i} - 1)}{\prod_{i \in S} (p_i^{n_i} - 1)} \cdot \sum_{\mathbf{z} \in (\mathbb{Z}^n)^* : (\bar{\mathbf{z}}_{\underline{p}})_i \neq \mathbf{0}, i \in S, (\bar{\mathbf{z}}_{\underline{p}})_{i'} = \mathbf{0}, i' \in \{S^c, K+1\}} f(\underline{\gamma}\mathbf{z}) \right] \end{aligned} \quad (39)$$

$$+ \left[\frac{(p_i^{k_{K+1}} - 1)}{(p_i^{n_{K+1}} - 1)} \cdot \sum_{\mathbf{z} \in (\mathbb{Z}^n)^* : (\bar{\mathbf{z}}_{\underline{p}})_{K+1} \neq \mathbf{0}, (\bar{\mathbf{z}}_{\underline{p}})_{i'} = \mathbf{0}, i' \in S^{(1)}} f(\underline{\gamma}\mathbf{z}) \right] \quad (40)$$

$$+ \sum_{S \subseteq \{1, \dots, K\}, S \neq \emptyset} \left[\frac{\prod_{i \in \{S, K+1\}} (p_i^{k_i} - 1)}{\prod_{i \in \{S, K+1\}} (p_i^{n_i} - 1)} \cdot \sum_{\mathbf{z} \in (\mathbb{Z}^n)^* : (\bar{\mathbf{z}}_{\underline{p}})_i \neq \mathbf{0}, i \in \{S, K+1\}, (\bar{\mathbf{z}}_{\underline{p}})_{i'} = \mathbf{0}, i' \in S^c} f(\underline{\gamma}\mathbf{z}) \right] \quad (41)$$

$$\rightarrow \frac{1}{((\tau_{K+1})^{n_{K+1}} - 1) \prod_{i \in \{S^{(1)}, K+1\}} V_{f(\Lambda_{C_i})}} \int_{\mathbb{R}^n} f(\mathbf{d}) d\mathbf{d} \quad (42)$$

as $p_i \rightarrow \infty$, $\gamma_i \rightarrow 0$ (Definition 5). Since f has a bounded support (f vanishes at infinity), with the definition of $(\mathbb{Z}^n)^*$, the first term in (38) vanishes for sufficiently large $\gamma_i p_i \rightarrow \infty$ as shown in [10], [17]. The terms in (39) also vanish by noting that at least one of elements of \mathbf{z}_{K+1} is equal to the multiples of p_{K+1} , which results in $f(\underline{\gamma}\mathbf{z}) \rightarrow 0$ in (39). The term in (40) follows similarly. Finally, the term in (41) approaches to (42) for $S = \mathcal{S}^{(1)}$, and vanish otherwise in a way similar to (39), (40), as $\gamma_i \rightarrow 0$ with $p_i^{n_i - k_i} \gamma_i^{n_i} = V_f(\Lambda_{C_i})$ fixed as in those [10]. From Definition 1, $V_f(\Lambda_{S_i})/V_f(\Lambda_{C_i}) = 2^{R_i LT} = (\tau_i)^{n_i}$, then (25 b) can be obtained from (42). Finally, (16) can be obtained from (25 b) by following the footsteps in [16].

D. Proof of (22)

Proof: For the K users, we use the self-similar nested lattice (Definition 1) where $\Lambda_{S_i} = \tau_i \Lambda_{C_i}$, $\tau_i = \lfloor \rho_d^{\frac{r_i}{2M_u}} \rfloor$ in order to satisfy the transmission rate constraint $R_i(\rho_d) \doteq r_i \log \rho_d$. The ensemble $\mathcal{E}_{\Psi, C^{Lo}}$ defined in the proof of Theorem 1 with $k_i = 1$ (Definition 5) is considered, on which the corresponding lattices ensemble is then expurgated in a way similar to that in the proof of Theorem 6 in [16]. We denote the expurgated ensemble of codebooks, C_{code} (i.e., $C_{\Psi^{one}}$ given the corresponding lattices in the expurgated lattices ensemble), as C_{code}^{exp} . Then the average error probability, $P_e(\rho_d)$ in (T1.20) of Table I, can be upper bounded by

$$P_e(\rho_d) \triangleq E_{C_{code}^{exp}, \mathbf{H}_{dst}} [Pr(Er|C_{code}, \mathbf{H}_{dst})] \leq Pr(O) + E_{C_{code}^{exp}, \mathbf{H}_{dst}} [Pr(Er, O^c|C_{code}, \mathbf{H}_{dst})] \quad (43)$$

where $Pr(Er|C_{code}, \mathbf{H}_{dst})$ is the probability of the event that given a $\{C_{code}, \mathbf{H}_{dst}\}$, not all users are correctly decoded at the destination and O denotes for the outage event set of \mathbf{H}_{dst} (\mathbf{H}_{dst} does not satisfy (15)). For the second term on the RHS of the inequality in (43), by averaging the term $Pr(Er, O^c|C_{code}, \mathbf{H}_{dst})$ over $C_{code} \in C_{code}^{exp}$ and then over $\mathbf{H}_{dst} \in O^c$, we will show

$$E_{\mathbf{H}_{dst}} [Pr(Er, O^c|\mathbf{H}_{dst})] \doteq Pr(O) \quad (44)$$

Following the steps similar to those in [10] and [16], considering a tuple of multiplexing gains, r_i , to meet a diversity requirement d for each user as in [20], given a \mathbf{H}_{dst} , we have,

$$Pr(Er, O^c|\mathbf{H}_{dst}) \leq (1 + \delta) \frac{\tau_{K+1}^{n_{K+1}}}{\tau_{K+1}^{n_{K+1}} - 1} \left(\sum_{S \subseteq \{1, \dots, K\}, S \neq \emptyset} \rho_d^{LT \sum_{i \in S} r_i} \left(\frac{KM_u + M_r}{|S|M_u + M_r} \right)^{(|S|M_u + M_r)LT} \cdot \det \left(\mathbf{I}_{2(|S|M_u + M_r)LT} + \left(\mathbf{H}_{dst}^{\{S, K+1\}} \right)^H \mathbf{H}_{dst}^{\{S, K+1\}} \right)^{-1} \right), \quad (45)$$

where $p_i \rightarrow \infty, \forall i$ and $\delta > 0$.

Let $Pr(O) \doteq \rho_d^{-d(\mathbf{r})}$. Although $Pr(O)$ does not necessarily guarantee the minimum outage probability, it suffices for the DMT analysis as indicated in [23]. The explicit formulation of $d(\mathbf{r})$ is generally difficult to obtain since the joint probability density function (pdf) of eigenvalues of $(\mathbf{H}_{dst}^{\{S,K+1\}})^H \mathbf{H}_{dst}^{\{S,K+1\}}$ is generally not easy to evaluate. However, from Theorem 3.2.17 of [24], it can be seen that the joint pdf of these eigenvalues is a continuous function. Therefore, by choosing a sufficiently large, but finite T , such that the term on the RHS in (45) decays fast enough, we can prove that $E_{\mathbf{H}_{dst}}[Pr(Er, O^c | \mathbf{H}_{dst})]$ is exponentially equal to $Pr(O)$ using the techniques similar to those in [10], [16], [20] and [23]. Together with (43), we obtain (22). Note the rate loss terms in (45) are exponentially negligible (independent of ρ_d) in the DMT analysis. ■

REFERENCES

- [1] D. Tse and P. Viswanath, *Fundamentals of Wireless Communication*. Cambridge University Press, 2005.
- [2] J. N. Laneman, D. N. C. Tse, and G. W. Wornell, "Cooperative diversity in wireless networks: Efficient protocols and outage behavior," *IEEE Trans. Inform. Theory*, vol. 50, no. 12, pp. 3062–3080, Dec. 2004.
- [3] K. Azarian and H. El Gamal, "On the achievable diversity-multiplexing tradeoff in half-duplex cooperative channels," *IEEE Trans. Inform. Theory*, vol. 51, no. 12, pp. 4152–4172, Dec. 2005.
- [4] G. Kramer and A. J. van Wijngaarden, "On the white gaussian multiple-access relay channel," in *Proc. IEEE Int. Symp. Inform. Theory*, Sorrento, Italy, June 2000, p. 40.
- [5] D. Chen, K. Azarian, and J. N. Laneman, "A case for amplify-forward relaying in the block-fading multiaccess channel," *IEEE Trans. Inform. Theory*, vol. 54, no. 8, pp. 3728–3733, Aug. 2008.
- [6] L. Sankaranarayanan, G. Kramer, and N. B. Mandayam, "Hierarchical sensor networks: Capacity theorems and cooperative strategies using the multiple-access relay channel model," in *Proc. First IEEE Conference on Sensor and Ad Hoc Communications and Networks*, Santa Clara, CA, Oct. 2004.
- [7] G. Kramer, M. Gastpar, and P. Gupta, "Cooperative strategies and capacity theorems for relay networks," *IEEE Trans. Inform. Theory*, vol. 51, no. 9, pp. 3037–3063, Sep. 2005.
- [8] K. Azarian, H. El Gamal, and P. Schniter, "On the optimality of ARQ-DDF protocols," *IEEE Trans. Inform. Theory*, vol. 54, no. 4, pp. 1718–1724, Apr. 2008.
- [9] M. Yuksel and E. Erkip, "Multiple-antenna cooperative wireless systems: A diversity-multiplexing tradeoff perspective," *IEEE Trans. Inform. Theory*, vol. 53, no. 10, pp. 3371–3393, Oct. 2007.
- [10] Y. Nam and H. El Gamal, "On the optimality of lattice coding and decoding in multiple access channels," in *Proc. IEEE Int. Symp. Inform. Theory*, Nice, France, 2007.
- [11] A. Murugan, H. El Gamal, M. Damen, and G. Caire, "A unified framework for tree search: Rediscovering the sequential decoder," *IEEE Trans. Inform. Theory*, vol. 52, no. 3, pp. 933–953, Mar. 2006.
- [12] M. O. Damen, H. El Gamal, and G. Caire, "On maximum-likelihood detection and the search for the closest lattice point," *IEEE Trans. Inform. Theory*, vol. 49, no. 10, pp. 2389–2402, Oct. 2003.
- [13] C. Hausl and P. Dupraz, "Joint network-channel coding for the multiple-access relay channels," in *Proc. Int. Workshop on Wireless Ad-hoc and Sensor Networks (IWVAN)*, New York, June 2006.
- [14] T. Wang and G. B. Giannakis, "Complex field network coding for multiuser cooperative communications," *IEEE J. Select. Areas Commun.*, vol. 26, no. 8, pp. 561–571, Apr. 2008.
- [15] R. Zamir, S. Shamai, and U. Erez, "Nested linear/lattice codes for structured multiterminal binning," *IEEE Trans. Inform. Theory*, vol. 48, no. 6, pp. 1250–1276, June 2002.
- [16] H. El Gamal, G. Caire, and M. Damen, "Lattice coding and decoding achieve the optimal diversity-multiplexing tradeoff of MIMO channels," *IEEE Trans. Inform. Theory*, vol. 50, no. 6, pp. 968–985, June 2004.
- [17] H.-A. Loeliger, "Averaging bounds for lattices and linear codes," *IEEE Trans. Inform. Theory*, vol. 43, no. 6, pp. 1767–1773, Nov. 1997.
- [18] R. Ahlswede, N. Cai, S. R. Li, and R. W. Yeung, "Network information flow," *IEEE Trans. Inform. Theory*, vol. 46, no. 4, pp. 1204–1216, July 2000.
- [19] U. Erez and R. Zamir, "Achieving $\log \frac{1}{2} \log(1 + \text{SNR})$ on the AWGN channel with lattice encoding and decoding," *IEEE Trans. Inform. Theory*, vol. 50, no. 10, pp. 2293–2314, Oct. 2004.
- [20] D. N. Tse, P. Viswanath, and L. Zheng, "Diversity-multiplexing tradeoff in multiple-access channels," *IEEE Trans. Inform. Theory*, vol. 50, no. 9, pp. 1859–1874, Sep. 2004.
- [21] B. Rimoldi and R. Urbanke, "A rate-splitting approach to the Gaussian multiple-access channel," *IEEE Trans. Inform. Theory*, vol. 42, no. 2, pp. 364–375, Mar. 1996.

- [22] U. Erez, S. Litsyn, and R. Zamir, "Lattices which are good for (almost) everything," *IEEE Trans. Inform. Theory*, vol. 51, no. 10, pp. 3401–3416, Oct. 2005.
- [23] L. Zheng and D. N. C. Tse, "Diversity and multiplexing: A fundamental tradeoff in multiple antenna channels," *IEEE Trans. Inform. Theory*, vol. 49, no. 5, pp. 1073–1096, May 2003.
- [24] R. J. Muirhead, *Aspects of Multivariate Statistical Theory*. John Wiley and Sons, 1982.